

Accepted Manuscript

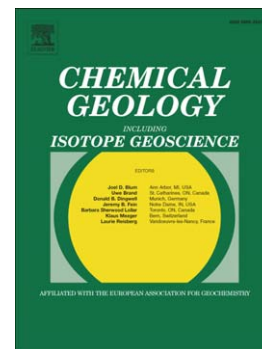
U-Th-Pb zircon geochronology by ID-TIMS, SIMS, and laser ablation ICP-MS: recipes, interpretations, and opportunities

U. Schaltegger, A.K. Schmitt, M.S.A. Horstwood

PII: S0009-2541(15)00076-5
DOI: doi: [10.1016/j.chemgeo.2015.02.028](https://doi.org/10.1016/j.chemgeo.2015.02.028)
Reference: CHEMGE 17506

To appear in: *Chemical Geology*

Received date: 17 November 2014
Revised date: 15 February 2015
Accepted date: 20 February 2015



Please cite this article as: Schaltegger, U., Schmitt, A.K., Horstwood, M.S.A., U-Th-Pb zircon geochronology by ID-TIMS, SIMS, and laser ablation ICP-MS: recipes, interpretations, and opportunities, *Chemical Geology* (2015), doi: [10.1016/j.chemgeo.2015.02.028](https://doi.org/10.1016/j.chemgeo.2015.02.028)

This is a PDF file of an unedited manuscript that has been accepted for publication. As a service to our customers we are providing this early version of the manuscript. The manuscript will undergo copyediting, typesetting, and review of the resulting proof before it is published in its final form. Please note that during the production process errors may be discovered which could affect the content, and all legal disclaimers that apply to the journal pertain.

U-Th-Pb zircon geochronology by ID-TIMS, SIMS, and laser ablation ICP-MS: recipes, interpretations, and opportunities

U. Schaltegger¹, A. K. Schmitt², M.S.A. Horstwood³

¹Earth and Environmental Sciences, Department of Earth Sciences, University of Geneva, Geneva, Switzerland (urs.schaltegger@unige.ch)

²Department of Earth, Planetary, and Space Sciences, University of California, Los Angeles, USA (axel@oro.ess.ucla.edu)

³NERC Isotope Geosciences Laboratory, British Geological Survey, Keyworth, Nottingham NG12 5GG, UK (msah@nigl.nerc.ac.uk)

Corresponding author:

Urs Schaltegger

Department of Earth Sciences

Rue des Maraîchers 13

1205 Geneva, Switzerland

email: urs.schaltegger@unige.ch

phone: +41 22 379 66 38

fax: +41 22 379 32 10

Abstract

The chronologic record encoded in accessory minerals, based on the radioactive decay of U and Th, is indispensable to extract quantitative process rates over timescales encompassing Earth's evolution from the Hadean to the Holocene, and extending from terrestrial to extra-terrestrial realms. We have essentially three different U-Pb dating tools at hand, a high-precision, whole-grain bulk technique (isotope-dilution thermal ionization mass spectrometry, ID-TIMS), and two high-spatial resolution but less precise in-situ techniques (secondary ion mass spectrometry, SIMS, and laser ablation inductively-coupled plasma mass spectrometry, LA-ICP-MS), all of which are predominantly applied to the mineral zircon. All three have reached a technological and methodological maturity in data quality and quantity, but interpretational differences, which are often common (albeit at different temporal and spatial scales) to all isotopic dating techniques, remain largely unresolved. The choice to use one of these techniques should be governed by the scientific question posed, such as (1) the duration of the geological process to be resolved; (2) the size and abundance of the material to be analysed; (3) the complexity of the sample material and of the geological history to be resolved; and (4) the number of dates needed to address the question. Our compilation demonstrates that, ultimately, the highest confidence geochronological data will not only result from the optimal choice of appropriate analysis technique and the accurate treatment of analytical and interpretational complexities, but also require comprehensive sample characterization that employs the full gamut of textural (e.g., cathodoluminescence, charge contrast imaging, electron backscatter diffraction) and compositional (e.g., trace element, stable and radiogenic isotope) analysis.

1. Introduction

Determining timescales of accessory mineral crystallization is critical for deciphering process rates in magmatic and metamorphic environments. Reconstruction of these processes must account for their non-instantaneous or repetitive nature: magmatic cycles can last over several 100 ka (e.g., Claiborne et al., 2010; Schoene et al., 2012) and hydrothermal activity and formation of ore deposits occurs in short events that collectively may last up to several 100 ka as well (e.g., Dalrymple et al., 1999; Chiaradia et al., 2013). Even for geologically young systems, it is, however, often challenging to discriminate between individual and repeated events. Because temporal resolution is inevitably coarser in deep geologic time, multiple high-frequency events are masked by a lack of age resolution and are integrated into quasi-continuous processes or instantaneous "events". Substantial efforts are undertaken to improve precision and accuracy of dating techniques to better meet the requirements of temporal resolution. As a consequence, analytical uncertainties approach the timescales of high-frequency events in magmatic and metamorphic environments and critical questions need to be addressed: What are the limiting factors of geochronological techniques – are they defined by the isotopic system, by the minerals we analyse, or by the analytical equipment we use? Where are the limits for interpreting a date (the numerical result of an isotopic analysis) as an age (the chronologic significance assigned to one or a series of dates) - are they inherent to open or complex isotopic system behaviour, due to our insufficient knowledge of how complex magmatic or metamorphic systems work in nature or is data quality and quantity an issue?

We will first review some recent innovations in both high-precision and high-spatial resolution U-Pb dating represented by chemical abrasion - isotope dilution - thermal ionization mass spectrometry (CA-ID-TIMS), secondary ion mass spectrometry (SIMS), and laser ablation - inductively coupled plasma mass spectrometry (LA-ICP-MS). CA-ID-TIMS represents the highest precision bulk dating method for zircon extracted from volcanic and plutonic rocks, whereas the two high-spatial resolution techniques SIMS (for U-Th disequilibrium dating of young volcanic zircon and for highest-spatial resolution geochronology of magmatic, metamorphic, and diagenetic crystal domains) and LA-ICP-MS (for magmatic, metamorphic, and detrital zircon; see Table 1) have wide applicability where bulk methods are limited by the internal complexity of the sample, by sample size or required data quantity. After summarizing key preparation and analysis procedures of the three U-Th-Pb dating techniques, we will discuss problems of both analytical-technical and

interpretational nature that have become obvious with increasing analytical precision and the understanding of process timescales gleaned from the study of active systems. An important aspect of this review is that key problems in interpreting accessory mineral geochronology are often similar or inter-related for the different methods, despite their differences in spatial and temporal resolution. We concentrate on the isotope systems of zircon as the main and most commonly used mineral for dating via the U-Pb decay systems, mainly because of its refractory behaviour throughout many geological processes, as well as the stability of its lattice even under conditions of high temperature and pressure. Other possible targets for U-(Th)-Pb geochronology abound, such as baddeleyite (ZrO_2 ; predominantly in mafic magmatic rocks), monazite (a light rare earth element [LREE] bearing phosphate; $[\text{LREE}]\text{PO}_4$), or titanite (CaTiSiO_5 ; ubiquitous in magmatic and metamorphic rocks), but these are only addressed for comparison, being aware that to be comprehensive, one would have to add a long list of these and other minerals found in magmatic, hydrothermal, and metamorphic environments where they are used with variable success and often lower precision than zircon. Ultimately we present working guidelines for the optimal use of the available dating techniques and data quality assurance, based on ongoing research, and provide an outlook for improving zircon geochronology to achieve enhanced reliability for data interpretation in a geologic context.

2. Current analytical and instrumental status and limitations

2.1. Chemical Abrasion - Isotope Dilution - Thermal Ionization Mass Spectrometry (CA-ID-TIMS)

2.1.1 Overview

The CA-ID-TIMS technique involves the separation of individual zircon crystals from a rock by either bulk methods or by extraction directly from rock sections. The material is then texturally, sometimes compositionally, characterized, pre-treated by chemical abrasion (Mattinson, 2005), and dissolved. The elements of interest - U, Pb, and (rarely) Th - are separated using chromatographic separation techniques in a very clean environment, and their concentrations and isotopic compositions analyzed by isotope dilution and thermal ionization mass spectrometry techniques (e.g., Parrish and Noble, 2003; Schoene, 2014). This technique yields the most precise and accurate U-Pb dates and is mainly applied to magmatic accessory minerals, predominantly to zircon.

In 2003, the U-Pb geochronology community started the EARTHTIME initiative (Bowring et al., 2005), which comprises more than 200 members from 30 countries and has gained widespread acceptance as a successful way forward to improve accuracy and precision of ID-TIMS U-Pb dating. Within this framework, jointly calibrated tracer and calibration solutions have been distributed to minimize the inter-laboratory bias due to different tracer calibrations (Condon et al., in review) and new software has been made available for the community, offering accurate handling of data and their associated uncertainties (Bowring et al., 2011; McLean et al., 2011b). Inter-laboratory bias exercises have shown that the differences between laboratories using EARTHTIME tracers have been reduced to 0.1% demonstrated by round-robin tests using natural zircon or by repeated analysis of synthetic solutions (Condon, 2005; Sláma et al., 2008).

The mineral-dissolution, isotope dilution technique, also termed "conventional", represents a multi-step procedure, which requires a high degree of control on many parameters to ensure highest data quality. Some of the most critical ones, outlining the most important innovations, will be addressed in the following paragraphs.

2.1.2 Sample pre-treatment by annealing and partial dissolution ("chemical abrasion")

The "chemical abrasion" treatment of selected zircon crystals prior to their dissolution involves annealing at 850-900°C, followed by partial dissolution in HF or HF-HNO₃ mixtures (Mattinson, 2005). It now has replaced the mechanical air-abrasion technique used since Krogh (1982). The treatment increases concordancy of ID-TIMS U-Pb dates by efficiently removing zircon domains that have a higher degree of damage due to the radioactive decay of uranium in the crystal, causing potential loss of radiogenic Pb.

Chemical abrasion increases precision and reproducibility but preferentially dissolves and removes U-rich zones, thus possibly biasing the result towards the age of the lower-U growth zones. Chemical abrasion may be applied collectively to a group of bulk separated zircon crystals, or individually to single crystals or crystal fragments extracted from an epoxy mount, following imaging and possibly in-situ chemical or isotopic analysis. Chemical abrasion techniques have been tested on some other accessory phases without clear evidence of improving concordance (e.g., baddeleyite, Rioux et al., 2010; monazite, Peterman et al., 2012).

2.1.3 Mass spectrometry

Isotope ratio analysis is performed on a thermal ionization mass spectrometer (TIMS), an instrument with a typical mass resolution of $M/\Delta M = \sim 500$ at 10% valley definition (Murray et al., 2013). This mass resolution does not allow for resolution of interferences (e.g., $^{138}\text{Ba}^{31}\text{P}^{17}\text{O}^{18}\text{O}$ on mass ^{204}Pb or ^{205}Tl interfering with the synthetic spike isotope ^{205}Pb), which therefore have to be monitored and appropriately corrected using mass 201 (which has a $^{138}\text{Ba}^{31}\text{P}^{16}\text{O}_2$ interference on it) and ^{203}Tl , respectively. Loading Pb onto a Re filament in conjunction with small amounts of a Si-gel activator and phosphoric acid produces long-lived ion beams of high stability that are mostly too small for Pb isotope analysis on Faraday collectors, but require the use of secondary electron or photo-multipliers in ion counting mode (Richter et al., 2001; Palacz et al., 2011). Mass spectrometric sensitivities of ID-TIMS (as well as for SIMS and LA-ICP-MS) are consistently expressed here as "useful ion yield" (or "useful yield" in short) which is defined as the number of detected ions of an isotopically pure species (atomic or molecular) divided by the total number of atoms of that isotope in the analyte mass. For ID-TIMS, the useful yield of Pb ranges between 1.6 and 6.4% using different Si-gels (Gerstenberger and Haase, 1997; Huyskens et al., 2012; Table 1). The best ion yields are generally obtained by depositing a thin layer of Si-gel made from silicic acid (Gerstenberger and Haase, 1997) onto the Re filament. Isotope ratio analysis by TIMS is routinely corrected for mass-dependent fractionation; a non-mass dependent fractionation component affecting the odd-valued ^{203}Tl , ^{205}Pb and ^{207}Pb isotopes has also been reported by Amelin et al. (2005) and McLean et al. (2011a). The U isotope composition is determined as UO_2^+ from the same Si-gel load used for Pb analysis, requiring knowledge of the oxygen isotope composition of the analyte loaded onto the Re filament, to correct for isobaric interference of $^{233}\text{U}^{18}\text{O}^{16}\text{O}$ on $^{235}\text{U}^{16}\text{O}_2$. UO_2^+ is analysed sequentially in ion counting mode or simultaneously with Faraday cups equipped with $10^{12} \Omega$ resistors. Using Faraday collection at low ion beam intensities requires accurate control of baseline intensity and stability, amplifier gain calibration and resistor decay rate.

The uncertainty in Pb isotope ratio determinations is composed of two major components: (1) the pulse counting statistic which is limited by the low ion beam signal measured on an ion counter ($\% = 1/\sqrt{N} \times 100$ where N = total number of counts); using multi-collection via an array of multipliers does not improve the precision, but adds the uncertainty of the multiplier cross-calibration to the counting statistics, and (2) the mass fractionation correction inherent to the TIMS source. No uncertainty is usually attached to the empirically determined dead

time of the multiplier, despite the well-known day-to-day fluctuations of secondary electron and photo multiplier tubes.

2.1.4 Uncertainty, accuracy, data treatment, and error reporting

A good knowledge of the sources of error is a prerequisite for intercalibration between different isotopic and non-isotopic (e.g., astrochronological) geochronologic techniques. Correct uncertainty estimation allows distinction between purely analytical data scatter and externally caused, excess data dispersion. It is also critical to avoid mistaking inter-chronometer bias such as between U-Pb and $^{40}\text{Ar}/^{39}\text{Ar}$ chronometers (e.g., Renne et al., 2010) for a real age difference. Later, we discuss briefly the different sources of uncertainty and error, a detailed and complete appraisal of which can be found in Schoene et al. (2013).

Zircon analyses may contain minute amounts of two types of Pb that are unrelated to U and Th decay: (1) Initial non-radiogenic Pb, commonly referred to as "common-Pb", is incorporated during crystallization. The uncertainty in the isotopic composition of the common lead correction (Pb_{com}) dominates the analytical uncertainty at low $\text{Pb}_{\text{rad}}/\text{Pb}_{\text{com}}$, and mainly affects the $^{207}\text{Pb}/^{235}\text{U}$ system. The isotopic composition of Pb_{com} may be estimated from the crustal growth model of Stacey and Kramers (1975) or from analysis of U-deficient minerals in the same sample, such as feldspars. Since most analyzed zircons contain very limited amounts of Pb_{com} , the $\text{Pb}_{\text{rad}}/\text{Pb}_{\text{com}}$ is mainly limited by the procedural blank. (2) Procedural blank Pb is introduced during chemical separation and analysis and can be distinguished from common-Pb by its different isotopic composition. State-of-the-art procedures may yield blank levels as low as 0.2 pg, including dissolution, ion chromatography and isotope analysis. Such low blanks are a pre-requisite to analyse small, low-U and/or young zircons at high precision. Accurate knowledge of the isotopic composition of the procedural blank component is essential at $\text{Pb}_{\text{rad}}/\text{Pb}_{\text{com}}$ ratios <5 ; the uncertainty on the isotope ratios used has to be propagated onto the final result. The effect of different Pb_{com} (isotopic composition) on two zircons with different $\text{Pb}_{\text{rad}}/\text{Pb}_{\text{com}}$ ratios is shown in Fig. 1a.

Insert here: Fig. 1

The accuracy of a U-Pb date determined by ID-TIMS is mainly determined by the accuracy of the tracer calibration, as well as by the U decay constant uncertainty. Prior to EARTHTIME, individually calibrated tracer compositions resulted in up to 1% inter-

laboratory bias on $^{206}\text{Pb}/^{238}\text{U}$ dates; the use of the (^{202}Pb -) ^{205}Pb - ^{233}U - ^{235}U tracer solutions distributed by EARTHTIME (ET2535 and ET535 tracers, respectively; www.earth-time.org) has now enhanced inter-laboratory reproducibility to better than 0.1% on $^{206}\text{Pb}/^{238}\text{U}$ dates. The tracer has been calibrated in different laboratories by using internationally certified, synthetic calibration solutions, and is controlled by analysis of international synthetic and natural reference materials (www.earth-time.org). The mass-dependent fractionation of unknown samples in the TIMS source may be quantified by repeated measurements of an international reference material (SRM 981, 982) but is for high $\text{Pb}_{\text{rad.}}/\text{Pb}_{\text{com}}$ analyses, preferably quantified and corrected internally by using the EARTHTIME double-isotope tracers for both U and Pb isotopes, taking into account potential isobaric and molecular interference on the two tracer masses ^{202}Pb ($^{138}\text{Ba}^{31}\text{P}^{16}\text{O}^{17}\text{O}$) and ^{205}Pb (^{205}Tl). A continuous control of reproducibility and accuracy has to be established in any laboratory through analysis of synthetic and/or natural reference materials. The EARTHTIME community has started to use synthetic solutions with apparent ages of 10, 100, 500 and 2000 Ma for the assessment of laboratory reproducibility (www.earth-time.org). Reproducibility can be evaluated by repeated analysis of well-characterized natural reference zircons, the most recent (CA)-ID-TIMS ages of which are compiled in Table 2. Repeated analysis of reference materials enables quantification of the long-term reproducibility for an isotope laboratory, and comparing results between different mass spectrometers and different multipliers, the latter requiring exchange every few years (in the case of secondary electron multipliers). An example of a representative dataset of the R33 reference zircon from the University of Geneva lab is shown in Fig. 2, demonstrating the complex nature of analytical work related to (1) poor analytical reproducibility requiring rejection of outliers due to dead time correction problems with the secondary electron multiplier (period 1), and (2) open system behaviour of natural zircon, attributed to insufficient or poorly reproducible chemical abrasion treatment prior to analysis (periods 2 and 3). This also demonstrates the difficulty of discriminating between analytical (multiplier performance) and natural sources (partial open system behaviour) of data scatter. Validation data from synthetic and/or natural materials should be included in any publication that is reporting high-precision U-Pb dates.

Insert here: Fig. 2

Additional factors to take into account are the values for the natural $^{238}\text{U}/^{235}\text{U}$ ratio in dated materials (Condon et al., 2010; Hiess et al., 2012) and of uranium decay constants (Schoene et al., 2006; Mattinson, 2010; Boehnke and Harrison, 2014). The latter is accounted for by

adding the decay constants' uncertainty band to the concordia curve in all concordia diagrams (Fig. 1). Be aware that for systems older than some 500 Ma, the $^{207}\text{Pb}/^{206}\text{Pb}$ ratio is the most precisely and reliably dated, at precisions of $\pm 0.02\%$ (e.g., Zeh et al., 2015).

Substantial discrepancies may be discovered when reducing isotopic data using different software packages, related to different correction and uncertainty propagation procedures. The EARTHTIME community has adopted an integrated open-source software infrastructure, interfaced with commercial mass spectrometers, for read-out and statistical filtering of the raw data ("Tripoli"), followed by a platform allowing for data reduction, correct uncertainty propagation and online data visualization ("UPb_Redux"; Bowring et al., 2011; McLean et al., 2011b). The final uncertainty of a U-Pb date is composed of several random and systematic elements. It is suggested that the community adopts the x/y/z notation proposed by Schoene et al. (2006; 2010a), [x] being the random (analytical) uncertainty, [y] containing the systematic uncertainty of the tracer calibration, while [z] also incorporates the U decay constant uncertainties (Table 1). The [x] uncertainty would be used when comparing data within the same or between laboratories using the same tracer solution, i.e., within the EARTHTIME community, [y] when comparing data based on different tracer solutions, and [z] when comparing U-Pb data with other chronometers such as $^{40}\text{K}/^{40}\text{Ar}$ (or $^{40}\text{Ar}/^{39}\text{Ar}$). Such an approach quantifying all random and systematic uncertainties is unfortunately not generally used in geochronology.

2.2 Secondary ion mass spectrometry (SIMS)

2.2.1 Overview

The unique strength of geochronological SIMS lies in its high spatial resolution and high useful yield or 'sensitivity' (Table 1). These merits result from the extremely shallow emission of target atoms and molecules dislocated by collisions with high-energy primary ions and ejected from a depth within a few nm of the surface. Ejected components include atoms from the target, the primary beam, and other sources (e.g., conductive coating, surface contaminants, residual gases in the vacuum). In-situ ionization of some of these species under ultrahigh vacuum conditions permits efficient ion collection. The high sensitivity of SIMS makes it the least destructive of the three analysis techniques described here, with the advantage that sufficient material is typically preserved to permit post-analysis geochemical, structural, or textural characterization. The flipside of the slow removal of material via

sputtering (e.g., sputter rates for zircon are $\sim 0.07 \mu\text{m}^3/\text{sec/nA O}^-$ at lateral beam dimensions of ~ 2 to $30 \mu\text{m}$ in diameter and beam intensities of $\sim 50 \text{ pA}$ to $\sim 100 \text{ nA}$; Fig. 3) are comparatively long analysis durations required to integrate sufficient counts, typically employing electron multipliers in mono- or dynamic multi-collection. Individual spot analyses may thus last at least several minutes, although 5 s duration rapid screening protocols have been successfully applied to Hadean zircons (Holden et al., 2009). Consequently, SIMS is optimal for dating “valuable” zircons and/or small-volume samples whereas high throughput detrital zircon needs are much better served by LA-ICP-MS.

Since the early 1970's, U-Th-Pb zircon analysis has become a routine geochronological application in many SIMS labs worldwide, with an expanding, yet mostly non-routine, spectrum of applications targeting other U-Th-Pb bearing minerals (e.g., apatite, allanite, baddeleyite, calcite, monazite, opal, perovskite, pyrochlore, rutile, titanite, uraninite, xenotime, or zirconolite). U-Th-Pb geochronology has overwhelmingly been the domain of large magnet radius mass spectrometers (SHRIMP, CAMECA ims1270/1280) that have the mass resolution required to resolve the complex mass spectrum resulting from sputtering materials without prior chemical purifications (cf. section 3.4). These instruments are operated by relatively few university or government agency labs, and frequently are employed to serve other demands besides geochronology such as stable isotope analysis.

2.2.2 Sample preparation requirements and analysis types

Traditional SIMS mounts are rounds 25.4 mm in diameter, not exceeding $\sim 5 \text{ mm}$ in thickness (Fig. 3). The useful area, however, is smaller (diameters of $\sim 22 \text{ mm}$ for SHRIMP and of $\sim 20 \text{ mm}$ for CAMECA) because the lip of the sample holder covers part of the mount and the step between the mount surface and the holder edge causes local distortions in the secondary ion extraction field. Bias in U-Pb elemental fractionation has been reported if targets are located too close to the edge (e.g., Stern and Amelin, 2003). More recently, 35 mm diameter mounts with larger analyzable surface areas and reduced isotopic fractionation near the mount edges have been developed (Ickert et al., 2008; Peres et al., 2012).

Insert here Fig. 3.

In most cases, separated crystals from a rock sample and reference materials are cast in epoxy, or pressed into a soft metal (e.g., indium) to make a mount that can be accommodated

in the ion probe sample holder. It is a critical requirement for SIMS that sample surfaces are perfectly flat, requiring euhedral crystal shapes for pressed crystals, or careful grinding and polishing. Moreover, the sample surface needs to be conductive, which is typically achieved by applying a high-purity Au coating. Sectioned grain mounts (Fig. 4) must be imaged prior to analysis to aid in targeting homogeneous domains in complex crystals (see section 4.1). *In-situ* analysis (within petrographic thin section) is accomplished by extracting regions of interest using a diamond drill or saw and mounting them together with pre-polished reference zircons. Because sample chambers in SIMS instruments can only hold one mount at a time, the practice of mounting standards closely spaced with the unknowns is highly recommended because every sample exchange may change the analytical conditions (e.g., by altering sample chamber vacuum, temperature, or the extraction potential).

Insert here Fig. 4

SIMS depth profiling takes advantage of the shallow emission of secondary ions, whereby atomic mixing and knock-on scrambles the target to several nm depth, depending on impact energy, angle, primary ion species, and target material (Hunter, 2009). Within these limits, changes in the secondary ion signal can be directly related to compositional variation with depth, once sputter equilibrium is achieved. To better discriminate against secondary ions contributed from the more slowly sputtered edges of the pit, the primary ion beam can be rastered or defocussed and secondary ions gated either electronically or (in CAMECA ims “ion microscope” instruments) through an aperture in the secondary ion path so that ions emitted from the center of the crater are preferentially detected. For meaningful geochronological depth profiling, the sample surface must be flat, and growth domains must be oriented perpendicular to the direction of sputtering and have lateral dimensions larger than the sampled region of the crater. Zircon lends itself to depth profiling because euhedral crystals can be aligned with (100) or (110) prism faces flush with the mount surface (Fig. 4), making it possible to date very thin magmatic, metamorphic, or diagenetic overgrowths on crystal surfaces. For many geochronology applications, in particular for dating young crystals, secondary ion signals need to be integrated to depth intervals larger than the theoretical achievable resolution to obtain meaningful age precision. Nevertheless, sub- μm depth resolution for analysis of zircon growth domains is possible, permitting unique insights into the timescales of magmatic or metamorphic crystallization (see section 4.2).

Scanning ion imaging (SII) is a third type of analysis where 2-D, or, if sequentially recorded images are stacked, 3-D isotopic mapping is achieved (Fig. 4). Lateral resolution is dependent on the size of the primary ion beam which is at a minimum between ~500 nm and 2 μm in diameter for Cs^+ (Ga^+) and O^- primary ion beams, respectively (e.g., Harrison and Schmitt, 2007), and ~10's to 100's nm for NanoSIMS (e.g., Hofmann et al., 2009). Because small primary beams correspond to low secondary ion intensities, SII analyses are generally applied to highly radiogenic samples, for example to localize ~100 nm-sized patches of unsupported high $^{207}\text{Pb}/^{206}\text{Pb}$ in Archaean zircon (Kusiak et al., 2013; cf. Valley et al., 2014). SII is also applied to augment other imaging techniques used to characterize zonation in the target material (e.g., backscattered-electron BSE or cathodoluminescence CL). Compared to BSE or CL imaging, SII has the advantage that it has the sensitivity to quantify trace element distributions (e.g., for Ti-in-zircon; Hofmann et al., 2009).

Direct ion imaging (DII) is a semi-quantitative technique available in CAMECA ims instruments (Fig. 4). Secondary ions are projected onto a stacked detector consisting of an ion-sensitive channel plate and an electron-sensitive phosphorescent screen. In DII, spatial resolution relates to aberrations in the secondary ion transmission (typically ~0.5 μm), and is thus independent of the primary beam dimensions. A practical application of DII is aiding primary beam targeting for small targets that are not readily visible in the optical (reflected light) imaging or establishing isotope or elemental maps of a sectioned mineral.

2.2.3 Inter-element ratio calibration: procedures and sources of bias

Pb-isotopic fractionation in SIMS was found to be largely insignificant, although a subtle instrumental mass fractionation (on average $+0.70 \pm 0.52$ ‰) has been reported for $^{207}\text{Pb}_{\text{rad}}/^{206}\text{Pb}_{\text{rad}}$ in zircon (Stern et al., 2009). Consequently, uncertainties for $^{207}\text{Pb}/^{206}\text{Pb}$ dates are predominantly determined by counting statistics, and assumptions regarding common-Pb (section 2.2.4). In contrast, useful yields for Pb and U species vary strongly, as a rule of thumb for zircon between ~1 % for Pb^+ and UO^+ , and ~0.1-0.2% for U^+ and UO_2^+ (note that Pb-oxides are practically absent). This requires a correction based on the calibration of relative sensitivity factors (RSF) using reference materials (e.g., Table 2). Moreover, the Pb^+/U^+ RSF co-varies with the relative abundance of U-oxide species which has long been harnessed to improve the Pb/U RSF calibration by determining working curves involving ratios of U atomic and oxide species (i.e., “two dimensional” calibrations reviewed in detail

by Ireland and Williams, 2003). Regardless of the preferred calibration model, the resulting ~1-3% (2σ) laboratory reproducibility of Pb/U RSF measurements on reference materials believed to be homogeneous (e.g., Jeon and Whitehouse, 2014) frequently exceeds that expected from counting statistics, and is a limiting factor for more precise SIMS analysis. In contrast, the RSF for ThO_x/UO_x (with $x = 0, 1$, or 2) is much closer to unity, typically between 0.9 (e.g., zircon; Reid et al., 1997) and 1.1 (e.g., allanite; Vazquez and Reid, 2004), and thus can be directly determined with a high level of confidence without resorting to a two dimensional calibration.

To accurately apply the Pb/U RSF calibration, it must be realized that compositional differences between reference materials and unknowns can cause RSF variations (the so-called “matrix effects”) which, if unrecognized, can lead to systematic errors for the unknowns. It is therefore paramount that reference materials and unknowns compositionally match as closely as possible. This is straightforward for minerals with simple stoichiometry (e.g., zircon, baddeleyite, or rutile), with the possible exception of high-U zircon (e.g., White and Ireland, 2012) and baddeleyite (Li et al., 2010). Minerals other than zircon (e.g., monazite) often show strong compositional variability and require careful matching between reference materials and unknowns (e.g., Fletcher et al., 2010). The analysis of high-energy secondary ions (at -20 to 30 eV offset) mitigates Pb/Th matrix effects for monazite, but comes at the expense of an order-of-magnitude decrease in useful ion yield (Hietpas et al., 2010).

Where correlations exist between U-Pb dates and U abundances, they appear to be related to radiation damage and metamictization because U-Pb determinations of young high-U zircon lacks a concentration bias (White and Ireland, 2012). These findings also support the long-held notion that intact crystallinity of the target zircons is a prerequisite for reliable SIMS geochronology (Ireland and Williams, 2003). The magnitude of the matrix effect has been described as instrumentation and tuning dependent (White and Ireland, 2012), but is broadly similar for different instrumental designs (Fig. 5). High-U zircons also display wider ranges in ion ratios used for calibration (e.g., UO^+/U^+) compared to reference materials with normal-U concentrations (e.g., Temora), but differences exist in the calibration behaviour of high-U and normal-U concentration reference materials on different instruments (Fig. 5). Regardless of these differences, unusual calibration parameters are often a first-order indication of problematic target zircons, and it is therefore recommended to always report the calibration parameters for references and unknowns.

Insert here Fig. 5

A second cause of calibration bias can result from variable ion yields as a function of the crystal orientation with respect to the incoming primary ion beam. These are known as “crystal orientation effects” and have been documented for baddeleyite (Wingate and Compston, 2000) and rutile (Taylor et al., 2012; Schmitt and Zack, 2012), but are not detectable for zircon and monazite (e.g., Wingate and Compston, 2000). Elevated oxygen surface concentration induced by a gas jet (O₂ flooding) pointing towards the sample surface demonstrably mitigates crystal orientation effects for baddeleyite and rutile (Schmitt et al., 2010; Li et al., 2010; Schmitt and Zack, 2012), while also boosting Pb⁺ ion yield of the CAMECA ion probes (Schumacher et al., 1994; Schmitt et al., 2010; Schmitt and Zack, 2012).

A common characteristic of any Pb/U RSF miscalibration, regardless of its origin (e.g., matrix or crystal orientation effects), is that it shifts data along a trajectory indistinguishable from modern day (Pb-loss) or reverse (U-loss or unsupported radiogenic Pb) discordance. As a consequence, miscalibration causes displacement of the analyses of old zircon at a steep angle to concordia. In the case of reverse discordance, this is readily identifiable as an analytical artefact. When young minerals are dated, instrumental bias introduces variation in U/Pb tangential to the slope of concordia which is more difficult to recognize as an artefact because it resembles minor Pb-loss or inheritance.

2.2.4. Common-Pb correction

Common-Pb corrections are critical in SIMS because of the small volume of material consumed which render Pb analyses vulnerable to surface contamination (especially affecting the accuracy of ²⁰⁷Pb/²³⁵U ages). The presence of non-radiogenic Pb (Pb_{com}) also causes displacement of data points off concordia, but their trajectory is controlled by the composition of ²⁰⁷Pb_{com}/²⁰⁶Pb_{com} (Fig. 1). Proxies for common-Pb (primarily ²⁰⁴Pb) typically show decreasing intensities with sputtering time, indicating that most non-radiogenic Pb is surface derived. At UCLA anthropogenic ²⁰⁷Pb_{com}/²⁰⁶Pb_{com} = 0.8283 (Sanudo-Wilhelmy and Flegal, 1994) is the default Pb composition for correcting zircon where common-Pb intrinsic to the crystal lattice is extremely low. Measures of common-Pb used to determine corrections are ²⁰⁴Pb (stable), ²⁰⁷Pb (quasi-invariant for young zircon; Baldwin and Ireland, 1995), or ²⁰⁸Pb (quasi-stable for zircon with high U/Th; Compston et al., 1984). The main causes for

erroneous common-Pb corrections are over- or undercounting of the monitor common-Pb species, in particular for ^{204}Pb . Undercounting can occur if peaks are mis-centered which can typically be avoided by using nearby reference masses for peak centering (e.g., $^{94}\text{Zr}_2\text{O}$ for ^{204}Pb). Overcounts can result from interferences that are unresolved at the mass resolution $M/\Delta M = \sim 4500$ at 10% valley definition routinely used for SIMS U-Th-Pb geochronology. Practically unresolvable interferences with their nominal mass resolution requirements in parenthesis are: $^{204}\text{Hg}^+$ (500,000), $^{232}\text{Th}^{144}\text{Nd}^{16}\text{O}_2^{++}$ (50,000), or $^{186}\text{W}^{18}\text{O}^+$ (11,000). With the exception of $^{204}\text{Hg}^+$ (sometimes due to contaminated Au targets used for applying the conductive coating), these interferences are much more detrimental for monazite (high Th) and rutile (high W) than for zircon. For monazite and rutile, peak-stripping from monitoring related species (e.g., $^{202}\text{Hg}^+$, $^{232}\text{Th}^{144}\text{Nd}^{16}\text{O}_2^{++}$, or $^{183}\text{W}^{18}\text{O}^+$, respectively) or the suppression of the interference using energy filtering can mitigate their impact on the common-Pb correction.

2.2.5 Data treatment and error reporting

No universally accepted protocol for SIMS data reduction exists, and software is generally tailored to the specific instrumentation operated by different labs. The diverse types of data (e.g., spot analyses, depth profiles, or ion imaging) further complicate standardized data reduction and reporting. In addition to the considerations about error hierarchies for ID-TIMS, uncertainty reporting for SIMS U-Pb ages requires an additional level because of the dependency on reference measurements and their analytical (random) and systematic uncertainties. Although age is primarily not a factor known to constitute calibration bias because Pb is characteristically present as a trace element below the levels that would cause matrix effects, it is highly recommended to analyze secondary zircon references of similar age as the unknowns under the same analytical conditions. This permits monitoring potential analytical artefacts (e.g., peak misalignments), and aids in constraining an adequate number of points analyzed for the RSF calibration curve whereby reference analyses should bracket the unknowns. Reporting dates for secondary references is thus a recommended practice which permits a first order assessment of data precision and accuracy.

2.3 Laser Ablation Inductively Coupled Plasma Mass Spectrometry (LA-ICP-MS)

2.3.1 Overview

With the first laser ablation U-Th-Pb dating studies being published ca. 20 years ago (e.g. Fryer et al. 1993, Feng et al. 1993), this technique is relatively new compared to TIMS and SIMS geochronology. Since these early studies, the major strength of the technique has been recognized in its flexibility and speed of data acquisition, making it ideally suited for studies requiring large datasets such as detrital mineral provenance (e.g. Machado & Gauthier, 1996; Pullen et al., 2014, and references therein) and detailed investigations into complexly zoned crystals (Gerdes and Zeh, 2009; Bosse et al., 2009). LA-ICP-MS can be applied to virtually any U containing material suitable for geochronology (apatite, allanite, baddeleyite, carbonate, monazite, rutile, titanite, uraninite, xenotime, zircon, and others), with the key limitation being the availability of homogeneous reference materials (e.g., Table 2). The method offers high lateral spatial resolution similar to SIMS, with typical spot sizes of 25-35 μm used for zircon geochronology, up to 50 μm for rutile work (having lower average U concentrations), and as small as 5 μm (though usually 10-15 μm) for monazite dating which is best performed *in situ* (in petrographic thin sections) to preserve the textural context of the mineral and its interpretation relative to other structural and geochemical information. Depth penetration during laser ablation is much higher than during SIMS analysis (see section 2.2.2), with ablation rates usually ranging from 0.35 to 1 $\mu\text{m}/\text{sec}$ (0.07-0.1 $\mu\text{m}/\text{pulse}$; depending on the fluence used) and total crater depths of 15-40 μm during a 30-60 sec analysis. These lower penetration depths are achievable routinely with higher yielding instruments and analytical set-ups and recent studies and techniques are pushing even these limits to shorter durations and lower analyte volumes, (e.g. Cottle et al., 2009, 2012; Johnston et al., 2009; Steely et al., 2014) including depth profiling with resolution on the order of 150 nm/pulse for a 1-2 μm deep ablation.

The field of LA-ICP-MS has been rapidly expanding, driven by recent major technological improvements in laser as well as ICP-MS instrumentation and the huge and still growing demand for dates on magmatic and detrital zircon. One thousand U-Pb analyses per detrital sample can now be collected efficiently (Pullen et al., 2014) and trace element (or other isotope) data can be collected from the same volume of material (see discussion in section 4.3). Several recent comprehensive reviews and workshop volumes have summarized the technical advances in the fundamental understanding of laser-sample interaction (laser wavelength and pulse width), particle transport issues (sample cell design and carrier gas), improvements in ion yield and reduction of elemental fractionation by modifications to carrier and auxiliary gases (e.g. Koch and Günther, 2011; Russo et al., 2013). The LA-ICP-

MS U-Th-Pb community has implemented these recommended improvement strategies for increasing ion yield, reducing laser-induced elemental fractionation and reducing ablated volume, in order to improve data quality. Currently the method limit is stuck at 2% (2σ) for $^{206}\text{Pb}/^{238}\text{U}$ (Košler et al., 2013) and approximately 1% (2σ) for $^{207}\text{Pb}/^{206}\text{Pb}$, reflecting inter-laboratory and methodological differences in the generated data (Hanchar, 2009; Košler et al., 2013). However, these limits have been the focus of the laser ablation community over recent years and it has been recognized that more consistent and better documented practices are needed to resolve their origin. Community derived recommendations for better practice have recently been described (see www.Plasmage.org; Bowring et al., 2013).

2.3.2 Laser system influences

Ablation Cell design: Possibly the most significant improvement to have impacted LA-ICP-MS U-Th-Pb geochronology in recent years is the recognition of the importance of ablation cell design on the acquired data. Two-volume cell designs are now standard in most commercial laser ablation systems improving ablation signal response time and profile, consistency of elemental signal and ratio quantification, signal-to-noise ratio and ultimately, precision of data (Müller et al., 2009). Ablation takes place within an inner cup with a smaller effective volume than the larger sample chamber and better controls the local gas dynamics, evacuating the ablated material more efficiently. Signal responses and gas flows across the larger sample chamber are harmonized, providing more consistent inter-element data, particularly important when reference materials are mounted separately to samples. These improved performance metrics have reduced the total ablation duration required and translate directly to improved spatial resolution in area but particularly in depth.

Laser wavelength and pulse width: A second major improvement in recent years has been the more universal adoption of the deep-ultraviolet wavelength (193 nm) laser ablation systems, providing better absorption of the laser energy by the materials of interest, resulting in cleaner and more reproducible ablations, producing smaller particles of more uniform size distribution. These smaller particles (<150 nm) ionize more effectively in the plasma improving signal response, signal and plasma stability, and repeatability of the analyses (Guillong et al., 2003). Recent developments have also seen a move towards using ca. 100 femtosecond pulse widths (Horn and von Blanckenburg, 2007, Koch et al., 2006, Shaheen et

al., 2012) rather than the more traditional 4-25 nanosecond pulse widths, in an effort to improve laser induced inter-element and isotopic fractionation. However, this has not yet shown significant improvement for U-Th-Pb data (d'Abzac et al. 2011; Koornneef et al. 2012) although the optimum wavelengths and pulse widths of femtosecond laser systems used for U-Pb dating have yet to be established.

2.3.3 Mass Spectrometry

Multiple collector (MC)-, single collector (SC)- and quadrupole (Q) ICP-MS are employed for U-Pb geochronology and achieve broadly the same results, at least with respect to the limiting Pb/U uncertainty. Some improvements in Pb isotope data can be achieved using MC-ICP-MS but newer very rapid scanning SC-ICP-MS instruments can achieve similar counting statistic precision, limited only by the dynamic range of the multiplier, due to their pseudo-simultaneous mode of operation. However, until improvements of the limiting Pb/U uncertainty can be realized, improved Pb isotope precision of one form of MS over another is of limited value since resolving concordance is constrained by the larger Pb/U uncertainty. Ultimately, single-collector detection will always be less precise than multi-collector detection for highly variable, low intensity and/or short duration ion beam signals even for the fastest scanning mass spectrometer systems. This is due to counting statistic limitations resulting from the short dwell times required during rapid scanning mass spectrometry and the non-simultaneous acquisition of the isotopes during rapid signal variations (spectral skew). However, more practical limitations complicate the optimal choice of ICP-MS for laser ablation analysis. For most routine U-Pb applications, a Q-ICP-MS system can achieve the same Pb/U uncertainties as the sector field instruments due to the laser ablation and ICP-based limiting uncertainties being greater than any spectral skew contributions when appropriate analysis routines are selected. However, this comes at the expense of greater sample consumption due to their lower ion yields, causing compromise in the spatial resolution of the analysis. Q-ICP-MS systems are also less able to reliably measure the low level ^{202}Hg and $^{204}(\text{Pb}+\text{Hg})$ peaks required for the correction of common-Pb. MC-ICP-MS systems are constrained by their limited dynamic range in their ion counting systems. Here, ion beams not much more than 1M cps (or those expected to reach this level in a small amount of time) cause protection mechanisms to 'trip' into place, ending the acquisition and generally causing loss of that analysis. Lower yielding SC-ICP-MS instruments are better

equipped to deal with such dynamic range variations by utilising quadrupole-like dual detection systems that switch rapidly from the pulse counting to analogue conversion range of the detector, thereby continuing the analysis. However, the calibration of this switch between the dual detection modes requires care to achieve accuracy and contributes an uncertainty usually in the percent range.

Great strides have been made in improving 'sensitivity' of mass spectrometers, coupled with the improvements in cell geometry mentioned above. The quotation of instrumental "sensitivity" varies across the ICP-MS community depending on what type of ICP-MS is being used (e.g. MHz or GHz per ppm concentration for SC and Q-ICP-MS, Volts per ppm concentration for MC-ICP-MS). However, all of these approaches require knowledge of the amount of material utilised to allow them to be compared. In the same way, signals derived by laser ablation on one instrument cannot be compared with another (or even between analyses from the same set-up on two different days), unless an ablation rate or total ablation pit volume is known.

Instrumental 'sensitivity' expressed as useful yield is independent of the method used to collect the data (Table 1). It is suggested that this be a new standard (*sensu stricto*) for reporting ICP-MS instrument performance with respect to signal response. Determination of nebuliser uptake rate is all that is required for solution analyses, with laser ablation analyses requiring determination of ablation rate per pulse at a particular laser fluence for a given mineral. Expressed in this way all ICP-MS instruments can be compared within and between laboratories, in wet plasma or dry, solution introduction or laser ablation, and compared to equivalent SIMS and ID-TIMS metrics for a much more informative evaluation. Typical useful yields for different instrument types are shown in Table 1 and better highlight their differential capabilities whilst noting that although similar yields might be achieved (e.g. SIMS; c.f. TIMS), the amount of material sampled constrains the overall achievable data precision. Hence, TIMS data are more precise than SIMS despite having equivalent yields and ICP-MS data can be as precise as SIMS but at the sacrifice of volume, despite having lower useful yields. For the best precision at the smallest volume though, nothing currently betters SIMS due to its comparatively high useful yields and small sampling volume.

2.3.4 Source of bias and overall uncertainty

One of the fundamental controls on U-Pb fractionation during laser ablation is the fluence used for ablation. Greater fluence (J.cm^{-2}) results in more ablation and therefore greater downhole fractionation of the measured Pb/U ratio. The ability to correct this and the uncertainty assigned to that correction, relies on the consistency of this fractionating profile. In a homogenous material, therefore, the consistency or repeatability of the laser fluence is critical to obtaining reproducible U-Pb data. As the community targets reduction of the U-Pb uncertainty, laser fluence repeatability and therefore fluence-induced Pb/U variation, will also need to improve. With increasing emphasis on single pulse, pulse-to-pulse and short ablation data analysis, laser fluence repeatabilities will need to be tightly constrained if they are not to become limiting to the achievable uncertainty. Ideally, it might be expected that the variability of Pb/U as a result of fluence repeatability, should be ten times lower than the overall target uncertainty to limit the impact of this parameter.

Laser-induced inter-element (or down-hole) fractionation (LIEF) is still one of the limiting analytical factors in LA-ICP-MS U-Pb dating. Combined with metamictisation, geochemical and structural alteration (of zircons and other accessory phases) affects the ablation rate of the material, varying LIEF within and between materials of the same nominal composition. This results in systematic inaccuracies in the determined sample or validation results when directly compared to a reference material. Since these structural and geochemical variations naturally occur, this effect can only be mitigated by reducing the degree of LIEF occurring in the first place. This principally requires the use of low laser fluence and/or larger spot sizes to prevent excessive depth penetration and restrict the aspect ratio of the ablation pit to less than 1:1, that is, a depth less than the spot size. This is more easily achieved therefore, by more 'sensitive' or efficient set-ups which achieve greater ion yields. The laser hardware and its specific optical design also impact the extent of LIEF and poor gas dynamics in the ablation cell and transport tubing can mask and overprint the true form of the LIEF, complicating its correction. Great care is therefore required to prevent these effects and to limit the degree of LIEF occurring.

One of the key problems for LA-ICP-MS U-Pb geochronology is the inability to precisely measure ^{204}Pb for the correction of common-Pb. Despite the time sacrifice (for SC & Q-ICP-MS systems) in doing so, we would like to advise that the two principal masses ^{202}Hg and $^{204}(\text{Pb}+\text{Hg})$ should be monitored in any case, even imprecisely, to allow recognition of common-Pb components clearly above background. Without this, the cause of discordant data points can only be surmised to be common-Pb rather than demonstrated. Ultimately

however, laser ablation is limited in its ability to correct for common-Pb when compared to both ID-TIMS and SIMS. Equally, ‘blind acceptance’ of common-Pb corrected data, without scrutiny of the data scatter prior to correction, can mislead interpretations due to masking of non-analytical scatter by the increased data point uncertainties after correction. In addition, false impressions of concordance may result as data are forced to the concordia by assuming potentially inaccurate common-Pb compositions for correction. This is potentially a problem at all scales of precision for each of the techniques described in this manuscript. Arguably a better way of assessing common-Pb affected data is to first view it without common-Pb correction on a Tera-Wasserburg ($^{207}\text{Pb}/^{206}\text{Pb}$ vs. $^{238}\text{U}/^{206}\text{Pb}$) diagram so that the true scatter in the data can be seen as well as the trend in the data indicating the appropriate composition to use for correction. Sometimes this trend is not visible within a cluster of data and the analyst has no option but to assume a relevant composition based on other information. However, particularly for non-zircon accessory phases, common-Pb compositional constraints may be determined from U-Pb data with excess scatter, by initial plotting of data that are not corrected for common-Pb, prior to the expansion of the uncertainties due to the correction, and thus allowing the smaller data point uncertainties to better resolve these components. Better resolution of the true scatter is important in defining whether the data do indeed represent a single population, the fundamental assumption which must be adhered to if the data are to be corrected. A common-Pb corrected age and uncertainty can then be more appropriately defined in this way. Equivalent to a ^{207}Pb -based common-Pb correction, this approach still ignores however, the potential for Pb-loss to also disturb the system, except in that Pb-loss in addition to common-Pb would likely result in increased scatter of the data population now better resolved with the uncorrected, more precise, data point uncertainties. Anderson (2002) highlighted the limitations of ^{207}Pb and ^{208}Pb -based common-Pb corrections in the presence of Pb-loss and illustrated an alternative approach, not requiring measurement of ^{204}Pb (particularly for ICP-MS-based measurements), which accounted for non-zero age Pb-loss within a data population. The potential for systematic errors after correction were however noted at Pb-loss proportions greater than a few percent.

2.3.5 Method work flow and data treatment

Imaging is a critical first step in the LA-ICP-MS U-Th-Pb workflow. Cathodoluminescence (CL), back-scattered electron (BSE), electron back-scattered diffraction (EBSD), elemental maps and other sample characterization methods are important tools allowing precise targeting of microbeam analyses and evidence-based interpretation of the data. Transmitted

light optical imagery is also useful for laser ablation work in conjunction with surface images, to avoid common-Pb bearing sub-surface cracks and inclusions which might otherwise be sampled during ablation. Ultimately the output data should be interpreted with the image information in hand so that aberrant data points can be considered in the context of their analysis position in the material, its complexity and the likelihood of encountering a problem with depth.

Recent community-based efforts have sought to minimise systematic artefacts in laser ablation U-Pb data to better understand their nature and determine appropriate data handling routines and uncertainty propagation protocols. This LA-ICP-MS U-Th-Pb Network has made recommendations for the appropriate handling, reporting and interpretation of LA-ICP-MS U-Pb data (www.Plasmage.org;) which should result in improved standards (*sensu stricto*) in this field of geochronology and lead ultimately to a reduction of the method limiting uncertainty, perhaps to as little as 0.5% (2σ) for the Pb/U ratio. The method limiting uncertainty reflects the community inter-laboratory comparison capability and requires sources of systematic errors (*sensu stricto*) to be identified.

Although new data handling procedures have been recommended, until such time as these become common-place amongst practitioners, variability of data treatment remains a fundamental limitation in this field of geochronology. Until improved uncertainty assessment is common practice, allowing better resolution and comprehension of data scatter, improvements to analytical and instrumental set-up will not be achieved and inter-laboratory comparison will remain at the ca. 2% (2σ) level.

3. Limits on the interpretation of geochronologic dates

3.1 Correction for initial ^{230}Th and ^{231}Pa disequilibrium

As a result of differing mineral-melt distribution coefficients (D) for the different elements present within the ^{238}U and ^{235}U decay chains, crystallizing accessory minerals exclude or enrich long-lived intermediate daughter products relative to their parent isotopes. For geochronology, the two most relevant nuclides are the comparatively long-lived ^{230}Th (half-life $t_{1/2} = 75,584$ a; Cheng et al., 2013) and ^{231}Pa ($t_{1/2} = 32,760$ a; Robert et al., 1969), which for zircon are enriched or depleted, respectively, relative to secular equilibrium. Magmatic processes do not fractionate ^{234}U ($t_{1/2} = 245,620$ years; Cheng et al., 2013) from its parent, but

recoil ejection and leaching can lead to ^{234}U loss and a resulting deficit in ^{206}Pb in radiation damaged minerals (e.g., Romer, 2003; Cheng et al., 2013). Corrections for initial disequilibrium require knowledge of the partitioning ratio between the U parent and a stable proxy X for the intermediate daughter D_X/D_U (Schärer, 1984). For ^{230}Th , X = ^{232}Th is used, with the Th/U of the melt estimated from the composition of whole-rocks, matrix glasses, or melt inclusions (e.g., Crowley et al., 2007). If melt or fluid compositions are unknown, experimentally or empirically derived D_X/D_U can be used (e.g., Blundy and Wood, 2003; Rubatto and Hermann, 2007). No stable proxy is available for ^{231}Pa , the longest-lived intermediate daughter in the ^{235}U decay chain. Lattice-strain partitioning models for the incorporation of $^{231}\text{Pa}^{5+}$ into the zircon lattice predict high K_D values (Blundy and Wood, 2003), which is in agreement with $D_{\text{Pa}/\text{U}} = 3.8 \pm 0.8$ determined from direct analysis of ^{231}Pa in late Pleistocene zircons and whole rocks (Schmitt, 2011). D_{Nb}/D_U or D_{Ta}/D_U zircon-melt values theoretically permit extrapolation to unsupported ^{231}Pa at the time of zircon crystallization, but this is confounded by uncertainties in the oxidation states of Pa and U (Burnham and Berry, 2012). To completely circumvent the problem of initial intermediate daughter disequilibrium, $^{208}\text{Pb}/^{232}\text{Th}$ ages can be determined. In that case, disequilibrium effects are negligible due to the short half lives of the intermediate daughters ($t_{1/2} < 5.75$ a; Mays et al., 1962), e.g., applied to hydrothermal monazite (Janots et al., 2012).

For complete ^{230}Th exclusion from the zircon lattice, the resulting correction amounts to a maximum of 110 ka on the $^{206}\text{Pb}/^{238}\text{U}$ date, using the ^{230}Th decay constant of Cheng et al. (2013). This is non-negligible for time-scale work in young, astronomically-tuned sedimentary sections, where the ^{230}Th disequilibrium correction may equal approximately four to five precession cycles (Wotzlaw et al., 2014). When applying a disequilibrium correction, initially distinct dates may converge (Fig. 1b). This example also illustrates that the Th disequilibrium correction effect becomes larger than the total $^{206}\text{Pb}/^{238}\text{U}$ age uncertainty for ID-TIMS dating of rocks < 100 Ma, and the estimated 50% uncertainty on D_{Th}/D_U becomes the dominant source of uncertainty for dates < 10 Ma (Wotzlaw et al., 2014; Fig. 1b). Zircon populations may show a large dispersal in Th/U ($^{208}\text{Pb}/^{206}\text{Pb}$) values that may reflect variable Th/U of the magma from which they crystallized, or a variable D_X/D_U of zircon at constant Th/U of the magma (see Rioux et al., 2012). For zircon, excess $^{207}\text{Pb}_{\text{rad}}$ will lead to erroneously old $^{207}\text{Pb}/^{235}\text{U}$ dates by up to 130 ka for D_{Pa}/D_U of 3.8 (Schmitt, 2011). This means that any zircon < 10 Ma will be measurably displaced to the right of concordia due to uncorrected ^{231}Pa excess (Fig. 1b).

3.2 Protracted crystallization of igneous zircon

3.2.1 Insights from U-series studies

How fast does zircon crystallize in natural systems, and what are the limits on the dating accuracy if the sampling volume integrates over diachronous crystal domains? U-series dating, mainly utilizing $^{230}\text{Th}/^{238}\text{U}$ disequilibrium, offers the highest absolute temporal resolution for recent crystals (e.g., Cooper and Kent, 2014). Moreover, SIMS depth profiles can interrogate crystal growth domains parallel to prism faces at sub-micron spatial resolution (Fig. 4). There is a growing data set for accessory minerals in youthful volcanic systems studied by U-series geochronology (e.g., Claiborne et al., 2010; Stelten et al., 2013), but for brevity we can only highlight results that bear directly on the interpretation of zircon ages. This is best done by focusing on a single study region, the Quaternary Taupo Volcanic Zone (TVZ) which embodies many characteristics of volcanic systems underlain by batholith-scale silicic magma bodies and which lends itself for a review because (1) its late Quaternary to recent age is ideal for high-temporal resolution U-series dating of zircon, (2) it preserves the products of high-frequency eruptions from multiple nested caldera systems, and (3) it has been studied by several research groups, thus providing an excellent opportunity to test different methodological approaches (Fig. 6).

Zircon populations from TVZ rhyolites and plutonic ejecta have been intensely studied by ID TIMS bulk and SIMS spot analysis, as well as SIMS studies using sectioned crystals and depth profiling of the outermost crystal margins (e.g., Charlier et al., 2003, 2005; Charlier and Wilson, 2010; Klemetti et al., 2011; Danišik et al., 2012; Shane et al., 2012; Storm et al., 2011, 2012; 2014), with results being largely complementary and mutually supportive. ID TIMS analysis of ~1 mg zircon separates comprising 100s of individual crystals for the Rotoiti eruption (~45 ka; Danišik et al., 2012) is in excellent agreement with the concentration-weighted SIMS average of multiple spots (~1 ng per spot; Charlier et al., 2003, 2005; Fig. 6). The stated precision of the TIMS age (approximately ± 2 ka), however, is geologically meaningless in the light of protracted crystallization (>300 ka) revealed by SIMS spot analyses (e.g., Charlier et al., 2003).

Insert here Fig. 6

Detailed depth profiling studies of zircon in post-Rotoiti rhyolites erupted from Tarawera volcano (TVZ) have revealed that zircon crystal rims frequently predate the eruption (Storm

et al., 2011; 2012). Moreover, individual crystals record protracted crystallization, which can be interrupted during recharge events due to increase of magma temperature and resorption of zircon. Tarawera data also reveal that, despite some actual heterogeneity of rim ages, the peak of the zircon rim age distribution progressively shifts towards younger age with decreasing eruption age. Statistical comparison of zircon age probability density distribution (PDD) curves further demonstrates that interior ages of the same population are indistinguishable from the rim ages of the preceding eruption (“Storm’s rule”; Fig. 6), implying that pre-existing zircon in unerupted residual magma is a preferred nucleation site for renewed crystallization. Trace element zoning within Tarawera zircons displays mostly normal, retrograde (down-temperature) crystallization trends indicated by rimward decreasing Zr/Hf and Ti (Fig. 7), but a significant (~30%) proportion of depth-profiled zircons indicate crystallization following thermal and compositional reversals (i.e., rimward increases of Zr/Hf and Ti; “recharge” in Fig. 7).

These observations collectively reveal that the zircon ‘cargo’ in volcanic rocks is sourced from heterogeneous domains in the magma storage region where zircon crystallization followed distinct thermal and compositional evolutionary paths. Moreover, the absence of near-eruptive aged rims in some crystals indicates that zircon residence in the host magma is often too short to directly record the conditions in the liquid-dominated, eruptible portion of a magma reservoir. In favourable instances, plutonic clasts excavated during pyroclastic eruptions provide additional insights into the compositional and thermal heterogeneity of long-lived magma reservoirs. Where zircons in plutonic rocks formed synchronously to those of their volcanic host, they have been interpreted as ripped up from highly crystalline mushes (e.g., Charlier et al., 2003), whereas in other cases plutonic zircons predate those in co-erupted volcanic rocks and may indicate an origin from older intrusive carapaces which acted as barriers to the interaction of magma with country rock, but also are a potential source of “old” zircons in subsequent eruptions (e.g., Shane et al., 2012).

The recognition of the complexity of zircon ages in young igneous rocks led to the classification of Miller et al (2007) who distinguished an *autocrystic* population (youngest grains that grew in equilibrium with the last magma batch in which they occur), and an *antecrystic* population that is derived from earlier stages of magma evolution within the same plumbing system and thus yielding older U-Pb dates (see example in Fig. 8), to be distinguished from *xenocrystic* (zircon that is accidentally entrained into the magma) or *inherited* zircon (derived from melting of a source rock). There are no clear boundaries

between these categories (Fig. 7). In particular, the difference between antecrystic and autocrystic growth (according to the definition of Miller et al., 2007) merits some more consideration: zircon is stable within a temperature window and a magma composition characteristic for melt saturation for this mineral (Watson and Harrison, 1983; Boehnke et al., 2013). This temperature may be repeatedly exceeded during recharge of a magmatic system by incoming hot magma, leading to resorption and partial dissolution of previously crystallizing zircon, followed by cooling down to temperatures of zircon saturation and crystallization. Repeated cycling through the saturation temperature band commonly lasts for a few 10's to 100's ka (e.g., Broderick 2013; Storm et al., 2011; 2012; 2014; Wotzlaw et al., 2013), reflected by multiple peaks in PDD curves from multi-episodic zircon growth (Fig. 8a, b). Because of the extended zircon crystallization in long-lived magma systems, zircon ages cannot *a priori* be interpreted to record an instantaneous geologic event, with implications for ID-TIMS dating discussed below.

Insert here Fig 7

3.2.2 Scattered zircon U-Pb dates from high-precision ID-TIMS dating of igneous rocks

The advent of the precisely calibrated EARTHTIME tracers, the chemical abrasion pre-treatment and the use of linear and stable electron and photo multipliers for ion counting of the minor Pb masses, has led to <0.1% precision on common-Pb corrected $^{206}\text{Pb}/^{238}\text{U}$ dates. The low $\text{Pb}_{\text{rad}}/\text{Pb}_{\text{com}}$ ratios, the uncertainty of the isotopic composition of the procedural blank and the possibility of a common-Pb component in the zircon, renders the $^{207}\text{Pb}/^{235}\text{U}$ date unreliable for Phanerozoic zircon (see Fig. 1b). The community focused on high-precision dating of igneous rocks has therefore shifted away from the concordia-age concept (Ludwig, 2003) and is using instead a statistical approach on the $^{206}\text{Pb}/^{238}\text{U}$ date only. The data are displayed as $^{206}\text{Pb}/^{238}\text{U}$ date-ranked distribution plots, and corresponding PDD curves (Fig 8). High-precision ID-TIMS dates are obtained from a whole volume or a (mostly randomly sampled) fragment of one single zircon grain, excluding only the decay-damaged zones that have been mostly dissolved during chemical abrasion. The date therefore represents an integrated history of crystallization over many growth zones. In the absence of radiogenic Pb loss or inheritance, dispersion of ID-TIMS dates therefore always give a *minimum* period for zircon crystallization in a given magmatic system. This approach implies removal of all discordance within the zircon volume that survived the chemical abrasion treatment, an assumption that cannot be proven in reality. Instead, perfect reproducibility within youngest

clusters of zircon dates, or coincidence with other chronometers such as U-Pb titanite, or astrochronology (Wotzlaw et al., 2014) are used as arguments to support this assumption.

Insert here Fig. 8

High-precision ID-TIMS U-Pb dating is predominantly applied to questions related to magma reservoir processes and for the reconstruction of the geological time scale, usually by dating volcanic ash beds in sedimentary sections. In the case of a volcanic ash or flow the aim is to date its eruption. The $^{206}\text{Pb}/^{238}\text{U}$ date of the youngest data cluster (assuming that it is not biased by Pb loss) is commonly adopted as an approximation of the age of the last crystallization; it then remains to quantify the time lapse Δt between the youngest zircon date and final solidification or eruption. High-precision U-Pb dating of volcanic zircon in 4 to 12 Ma old ash beds from astrochronologically well-characterized upper Miocene sedimentary successions demonstrates that in some cases Δt cannot be resolved because it is therefore smaller than our analytical uncertainty of 4 to 12 ka; at the other extreme the Δt may reach a few 100 ka (Wotzlaw et al., 2014). This means that for volcanic rocks >100 Ma, Δt is largely negligible relative to analytical uncertainties.

The total dispersion of U-Th or $^{206}\text{Pb}/^{238}\text{U}$ dates in a zircon population characterizes the temporal and spatial heterogeneity of magma bodies which may alternate between near-solidus and partially re-molten states, and which are open to thermal and compositional rejuvenation via magma recharge (e.g., Wotzlaw et al., 2013; Storm et al., 2014). Although the dynamics of such magma systems are not entirely understood, it is conceivable that liquids carrying suspended zircons (and other fine-grained minerals) separate from coarser-grained solids, and that melt-zircon suspensions are transported towards higher crustal levels due to buoyancy overpressure. Consequently, zircon age dispersion may not necessarily record protracted zircon growth in a melt batch undergoing closed-system crystallization, but may result from zircon crystallization in melts that were saturated at different times and that were intermittently stored under conditions close to the magma solidus (Broderick, 2013; Cooper and Kent, 2014). Based on thermal considerations, the time taken for effective solidification at the level of final emplacement in the middle or upper crust is expected to be one or two orders of magnitude shorter than the age dispersion of plutonic zircon populations. The interpretation of zircon U-Pb ages in volcanic and plutonic systems may therefore be very complex; zircon may be recycled from precursor mushes and crystallize at any time the melt is zircon-saturated, be it during magma transfer through the crust, at emplacement, or

even during final cooling to the solidus and possibly hydrothermally under sub-solidus conditions. A plutonic zircon date therefore marks simply a transient stage of "rheological freezing" of a magma mush. The PDD curves derived from the distribution of $^{206}\text{Pb}/^{238}\text{U}$ zircon dates have been demonstrated to be related to magma volume and flux (Caricchi et al., 2014) and may be used for quantitative modelling of these parameters.

A concern for representative sampling of a population is the number of grains analyzed. This is generally more critical for CA-ID-TIMS dates where the time and effort to carry-out individual analyses significantly exceeds that for SIMS or LA-ICP-MS, especially in cases of obviously complex zircon populations. Experience shows that 10-20 analyses are needed to interpret a complex population with sufficient confidence; if applied as a chronostratigraphic tool to a sedimentary succession, a high sample density is required in addition, to recognize complex magmatic behaviour of the U-Pb system in zircon (Guex et al., 2012; Wotzlav et al., 2013, 2014).

3.3 Scattered vs. clustered U-Th-Pb dates: data point precision and uncertainties on average ages

Irrespective of the analytical method, the uncertainty in individual isotopic measurements or data points determines one's ability to resolve scatter within a data set and to discriminate one data population from another. Most samples of volcanic and plutonic rocks contain zircons with a range of dates that may or may not be resolvable, depending on the uncertainty of the technique used (see, as an example, the history of U-Pb dating of the Fish Canyon Tuff; Schmitz and Bowring, 2001; Bachmann et al., 2007; Wotzlav et al., 2013). In order to evaluate whether the scatter may reflect solely analytical uncertainty, in which case it would be appropriate to calculate a weighted mean $^{206}\text{Pb}/^{238}\text{U}$ age, or whether it contains a component of excess scatter, the mean square weighted deviation (MSWD) is evaluated. For a large number of analyses, a $\text{MSWD} \approx 1$ (with the exact range of permissible values calculated from the number of analyses N averaged in the calculation; Wendt and Carl, 1991; Mahon, 1996) indicates scatter from analytical uncertainty only and/or has scatter unresolvable at the level of the assigned data point uncertainty (Kalsbeek, 1992). By calculating a weighted mean age we imply that all zircons have crystallized simultaneously within analytical resolution, or that any age difference remains unresolved within uncertainty. Zircon populations with excess scatter will yield unacceptably high MSWD values at a given

N and have to be interpreted in terms of real age dispersion (or open system behaviour) after any analytical bias has been ruled out. It is important to emphasize that even for zircon populations with no analytically resolvable scatter (i.e., MSWD = 1), it would be fallacious to interpret the limits of the uncertainty-weighted average as an indication for the actual duration of zircon crystallization. It is the analytical uncertainty of the individual measurements which dictates the capability to define a single population, and one may not *a priori* assume homogeneity in the population below this limit.

In addition it should be noted that a single population of data validated by MSWD statistics does not preclude a systematic error (i.e. bias) being present within the dataset. Sample results using a relative method cannot therefore be any more accurate (i.e. including precision) than the level to which the relevant reference materials are defined. Therefore, one of the fundamental limiting uncertainties for SIMS and LA-ICP-MS is the uncertainty in the composition of the reference zircon being used (Table 2). Systematic uncertainties (e.g., from tracer calibration in the case of ID-TIMS, or from decay constant determination) do affect data accuracy despite apparent high precision, and need to be propagated into final uncertainties when comparing between data from different techniques or to data from other chronometers.

3.4 Efficiency of chemical abrasion in ID-TIMS, SIMS, and LA-ICP-MS

The approach of focusing on the youngest sub-population of zircon grains requires that any trace of post-crystallization radiogenic Pb loss has been removed during the chemical abrasion treatment (Mattinson, 2005). There remains, however, the suspicion that a residual Pb loss component can influence the U-Pb date of the youngest zircons in a population, predominantly in ash beds that suffered post-depositional fluxing by aqueous solutions and volatiles. Whether a given analysis is biased by residual Pb loss or not is often a subjective decision. Failure to report such data in the data table of a scientific publication is poor practice that prevents eventual re-assessment of previously erroneously interpreted data.

Since chemical abrasion is a purely empirical procedure, it may be desirable to develop proxies in the future to detect minor traces of Pb loss. In addition, we need to be aware that chemical abrasion is preferentially removing the zones richest in U, thus biasing the U-Pb data towards, marginal or more internal, low-U growth zones (Fig. 7). How can “pathologic” behavior of the U-Pb system (e.g., Pb-loss, inheritance, and to minor extent initial

disequilibrium) be distinguished from true variations in crystallization age, and how much bias do we actually introduce through chemical abrasion? The high degree of reproducibility of chemically-abraded zircon dates in inter-laboratory cross-calibrations on natural zircon populations suggests that we can be rather optimistic in this respect, if we respect the limiting parameters and analyse a sufficient number of zircon crystals. These studies, however, employ mostly high-quality materials that have been proposed as international reference materials, which more easily reproduce their high-precision age.

A number of studies have now also identified the potential utility of thermal annealing or chemical abrasion for SIMS (Kryza et al., 2012) and LA-ICP-MS (Allen and Campbell, 2012; Marillo-Sialer et al., 2014; Crowley et al., 2014; von Quadt et al., 2014). Most studies demonstrate reduced ablation rates for thermally annealed or chemically abraded material when compared to ablation rates in untreated materials and improved concordance (reduced Pb-loss/common-Pb effects) of final results. Allen and Campbell (2012) cite the annealing of alpha recoil tracks and structural harmonization as the mechanism for a reduced ablation rate and improved validation to better than 1% accuracy, whilst Marillo-Sialer et al. (2014) indicate that the relative deviations between validation materials remain after annealing although ablation rates are reduced. Crowley et al. (2014) recognise reduced ablation rates even for Archaean zircons despite the mineral structure becoming more porous after widespread partial dissolution after chemical abrasion and von Quadt et al. (2014) also illustrate reduced Pb-loss effects, greater geological accuracy of the results and improved precision due to a reduction of scatter within the chemically abraded data populations.

However, since both SIMS and LA-ICP-MS techniques are described as requiring compositional and structural homogeneity between sample and reference materials to obtain appropriate calibrations, the indiscriminate application of chemical abrasion preparation procedures for samples could lead to increased variability in both parameters relative to the reference materials. Unless extensive unleached (low U) portions of the sample crystal are preserved, the dissolution part of the chemical abrasion procedure may result in extensive structural differences between samples and reference materials, exacerbating the variability of ablation rates and indeed increasing it significantly. Clearly then chemical abrasion and/or thermal annealing has a significant role to play in improving the method uncertainty limit and overall accuracy of SIMS and LA-ICP-MS U-Pb dates, but greater clarification of the effects of this approach are still required not least to ascertain the effect for complex zircons with multiple age domains which might be removed by the abrasion process. The value of high

spatial resolution techniques is in illustrating the presence of such previously unrecognised domains whilst attempting to date them. Their removal prior to their recognition could be considered a backward step.

It should be noted that for zircon dated by high spatial resolution techniques from material that is not pre-treated by chemical abrasion techniques it is not appropriate to apply the common strategy used by CA-ID-TIMS specialists to adopt the youngest analysis as a proxy for the last crystallization event in a magma, because such a date is potentially biased by Pb loss. In the same way, single laser ablation or SIMS analyses from detrital zircon spectra should not be used to interpret the maximum depositional age of sediments. This is best estimated from the average of multiple young dates overlapping within analytical uncertainty (Dickinson and Gehrels 2009; see recommendations on www.Plasmage.org) and regardless of whether CA pre-treatment was applied or not.

3.5 Reference materials

SIMS and LA-ICP-MS U-Th-Pb dating are comparative methods dependent on reference materials for determining RSF values for inter-element ratio corrections. They therefore require suitable natural or artificial reference materials, of similar elemental concentration and structural state to the unknowns, homogenous in age and ideally also Th/U and trace elements. There are currently very few well-characterized reference materials available (Table 2) and many with insufficient ID-TIMS age control. This limitation means that a SIMS or LA-ICP-MS date can only be as good as the homogeneity of the reference materials, the accuracy and precision to which such material is known, as well as the stability of the system during analysis (see section 3.3; Table 2). Some materials are well defined at ca. 0.1% ([x] uncertainty; 2σ) of their $^{206}\text{Pb}/^{238}\text{U}$ age (e.g., Plešovice, Sláma et al., 2008, or AUSZ2, Kennedy et al., 2014). For other materials, e.g., the Mud Tank zircon (Black and Gulson, 1978) and many of the monazite, rutile and titanite reference materials, this can be as bad as 3-4% (2σ , $^{206}\text{Pb}/^{238}\text{U}$ age). Concerning homogeneity, some of these “candidate reference materials” are far from being ideal, especially for non-zircon phases, but are simply all that is available. There is also a dearth of well-characterized Quaternary reference materials, where analytical challenges are highest because of low signals, crystallization age heterogeneity and initial isotopic disequilibrium.

The Plešovice zircon was demonstrated to perhaps have some age and/or matrix variation impacting on SIMS dates and likely also consistency of laser ablation results (Sláma et al., 2008). U variations within Plesovice crystals are as high as 465-3084 ppm, resulting in metamict areas with increased ablation rate and therefore downhole fractionation. The GJ-1 zircon appears very homogeneous for age within one crystal but different crystals are claimed to have slightly different ID-TIMS reference U-Pb ages (Jackson et al., 2004; Schaltegger et al., unpubl., in Boekhout et al., 2012).

It should be ensured that relevant reference values are used in reference to the relevant sample value. Comparing the Pb/U result for a material to its expected concordia age for example, is invalid and gives a false impression of accuracy, positively or negatively. Since few of the known ‘candidate reference materials’ for in situ U-Th-Pb geochronology, are concordant within the precision limits of the reference data (e.g. GJ-1, 91500), comparison of the correct reference ratio with the equivalent sample ratio is imperative. This is particularly important for non-zircon accessory phases which are increasingly the focus of research. Apatite (Chew et al., 2011; Thomson et al., 2012), rutile (Kooijman et al., 2010; Zack et al., 2011; Schmitt and Zack, 2012), titanite (Storey et al., 2006) and monazite (Harrison et al., 1995; Košler et al., 2001; Hietpas et al., 2010) all incorporate initial Pb to greater or lesser extents and commonly contain excess ^{206}Pb due to incorporation of excess ^{230}Th during crystallization. Reference values reflecting the exact composition of the material sampled are therefore required.

Ultimately, at the smallest scale, no reference material will be compositionally or structurally matrix-matched to an unknown. Recent individual and community efforts have attempted to compile a list of available reference materials for laser ablation U-Th-Pb geochronology. The Arizona LaserChron Centre (<https://sites.google.com/a/laserchron.org/laserchron/>) and the LA-ICP-MS U-Th-Pb Network (www.plasmage.org) detail lists of materials, their availability and origin.

3.6 Zircon U-Pb precision in comparison with other accessory minerals

As shown above, minerals other than zircon - with the exception of monazite, xenotime and baddeleyite - have distinctly lower $\text{Pb}_{\text{rad}}/\text{Pb}_{\text{com}}$ ratios and therefore cannot yield U-Pb dates at the same level of precision as zircon (see, e.g., Schoene et al., 2012). Correct uncertainty propagation of the isotope composition used for Pb_{com} correction is essential to obtain an

accurate $^{206}\text{Pb}/^{238}\text{U}$ age with correct associated uncertainty from these minerals. An optimized approach is to measure Pb_{com} in low-U phases such as feldspars and assume equilibrium with crystallizing zircon, instead of blindly using a model isotope composition from the crustal growth model of Stacey and Kramers (1975), evidently not possible for detrital minerals. For assessing the uncertainty of the Pb_{com} isotope composition, we can propagate the analytical uncertainty from the feldspar analyses, or model uncertainty limits taking the most extreme Pb_{com} isotope compositions found in the studied rocks. The application of the 3D isochron approach may evidence non-common, slightly radiogenic initial Pb isotope compositions, but is biased by the fact that, e.g., titanite crystallizes over a significant time span and therefore different single grains are not strictly coeval (Schoene et al., 2012).

Additional complication is presented in the case of baddeleyite which often shows effects of post-crystallization lead loss. Chemical abrasion or leaching treatment prior to analysis proved to be inefficient and leads to analytical artifacts (Rioux et al., 2010); the accuracy of baddeleyite and zircon data is therefore often not entirely equivalent.

High-precision monazite dating is hampered by initial ^{230}Th disequilibrium leading to unsupported radiogenic ^{206}Pb , which cannot be corrected in a metamorphic environment since the Th/U of the crystallizing medium is not known. This obstacle may be overcome by using the $^{207}\text{Pb}/^{235}\text{U}$ date at marginally lower precision, or to use the $^{208}\text{Pb}/^{232}\text{Th}$ isotopic systems instead, especially for SIMS and LA-ICP-MS.

4. Improving the interpretation of geochronologic data

4.1 Imaging and texturally controlled sampling

Cathodoluminescence (CL) imaging for zircon, back-scattered electron (BSE) imaging and electron probe elemental maps (for monazite and other accessory phases with complex chemical zoning) are essential aids for guiding selection of analysis locations for high spatial resolution dating studies (and increasingly for selecting crystals or crystal domains for high-precision ID-TIMS analysis) and help enable robust interpretations of U-Th-Pb data. Without knowledge of what is being analysed, a result, however precise, is less meaningful or even non-interpretable. Increasingly, techniques such as electron back-scattered diffraction (EBSD; e.g., Moser et al., 2009; Fig. 9a), SIMS ion imaging (e.g., Kusiak et al., 2013), charge

contrast imaging (CCI; Watt et al., 2000; Fig. 9b), Raman spectroscopy (e.g., White and Ireland, 2012), and transmission electron microscopy (TEM; e.g., Dobrzhinetskaya et al., 2014) are also coming to the fore, demonstrating the relationship between structural coherency of the material, crystal orientation, inclusions, contamination, and the significance of geochronological data.

The combination of imaging methods and U-Th-Pb age data, in providing compositional and structural variation information related to age, provides for much more powerful interpretations and better quality control of data. When consulted during data interpretation, imaging can help distinguish between isotopic results that are biased by lead loss and inheritance (or antecrystic zircon growth). However, although CL imaging is most prevalent, distinct boundaries between CL zones do not necessarily correlate with detectable age differences within a grain, locations of disturbance, or thermochemical boundaries. Conversely, zircon crystallization hiatuses have been documented by U-Th dating in young magmatic systems where CL images show no obvious discontinuities (Storm et al., 2011).

Insert here Fig. 9

While CL often gives a qualitative idea about the degree of complexity of the growth structures, other imaging techniques can reveal more reliable insights into the crystal structure (e.g., EBSD) and zonation (e.g., CCI). Moreover, repeated recharge of a magmatic system with increased temperature may lead to periods of dissolution (resorption) followed by growth again when saturation conditions are achieved. This leads to very complex internal textures of magmatic zircon formed over timespans that may not be resolved by high-precision ID-TIMS dating and whose detection may require ultrahigh-spatial resolution techniques such as depth profiling (e.g., Fig. 7).

4.2 In-situ and ultra-high spatial resolution analysis

High-spatial resolution techniques can directly target crystals in polished petrographic sections (*in situ* analysis *sensu stricto*). In-situ dating offers several advantages: (1) preservation of textures and context (e.g., linking metamorphic textures and parageneses to accessory mineral growth; Foster et al., 2004; Möller et al., 2003; Catlos et al., 2002); (2) accessibility of micro-crystals, inclusions, or epitaxial overgrowths which are otherwise difficult or impossible to separate (e.g., micro-baddeleyite; Schmitt et al., 2010; micro-zircon; Ault et al., 2012; diagenetic zircon overgrowths; Rasmussen, 2005); (3) avoiding

contamination (Hellebrand et al., 2007) and (4) the possibility to target armoured crystals which may be protected from later fluid events that mobilized Pb in radiation damaged crystals (e.g., Ault et al., 2012; Fig. 10). To facilitate targeting and minimize sample changes, pieces from the sections are cut or drilled out, and mounted together with pre-polished reference grains for SIMS, or for laser ablation multiple thin sections are simply loaded into the larger sample chamber. If micro-crystals are analyzed, laser or ion beam overlap onto adjacent minerals with high common-Pb potentially reduces radiogenic yields, but this can be mitigated through a more constrained sampling beam, i.e., use of a smaller laser spot size or, in the case of CAMECA ims instruments, narrowing secondary beam apertures (“field” and “contrast” apertures; Figs. 4 and 10) to preferentially select ions from the interior of the crater and ions with a near-perpendicular take-off angle, respectively.

Of course one disadvantage to *in situ* analysis of materials in thin section is that they cannot be treated using chemical abrasion to reduce Pb-loss. The potential for Pb-loss to affect the data has therefore to be taken into consideration during the interpretation of *in situ* data. However, the added benefit of textural context may outweigh the potential for complications from Pb-loss in the case of zircon data and for some accessory mineral data (e.g. monazites), data interpretation is virtually useless without petrographic context and Pb-loss problems in monazites are considered to be minimal.

Insert here Fig. 10

Depth profiling of zircon by SIMS (e.g., Fig. 11; Vorhies et al., 2013) or single-shot LA-ICP-MS (Cottle et al., 2009) is a viable technique revealing age variations on the 100 nm scale. Addition of tiny zircon layers during metamorphism was investigated by Vorhies et al. (2013) on detrital zircons from the Barrovian Complex (Scotland; see Fig. 11) where SIMS depth profiles of grain faces revealed thin (often <1 µm) zircon rims with low Th/U in greenschist to K-feldspar-sillimanite grade rocks. Only zircon from the highest grade rocks produced rims and marginal domains >10 µm in thickness that could be detected by conventional spot analysis on sectioned crystals. However, as discussed in Cottle et al. (2009), surface analysis of zircons using depth profiling methods to reveal ages of the crystal rim are prone to Pb loss and common-Pb effects. For young material (<100 Ma), the Pb-loss trajectory is tangential to the concordia curve and indistinguishable from concordance at the uncertainties of microprobe data. These data therefore need considered interpretation to take such factors into account.

Insert here Fig. 11

4.3. Combining data sets from different techniques and analytical approaches - Harnessing the full potential of high spatial resolution and high-precision methods

Ultimately, one of the factors limiting the accuracy of U-Pb data interpretation, is the quality and nature of the data themselves. Our ability to discriminate between two similarly aged materials or data points within data sets, is greatly increased by combining these data with other information. The complexity of accessory minerals at sub-grain to population level precludes any automation in date interpretation, but requires careful evaluation of additional and independent, chemical and physical information from the analysed material, to arrive at an accurate interpretation. Structural and chemical image analysis, or trace element and isotope chemical composition, add additional information upon which to base an assessment of single population status or exclude data points from the calculation of an average. The best, most robust dates will have proven their single population status through independent information (e.g., co-registered trace element or isotopic analyses) rather than ‘blindly’ assuming it based only on the MSWD statistic of the U-Pb data. In addition, high-precision and/or high-spatial resolution geochronology can now ‘map out’ changing processes such as magmatic differentiation and the crystallization history of a complexly zoned zircon and allow interpretation of the rate of chemical and geological evolution.

Trace element information can help to characterize the crystallization history of zircon in different evolving melt batches over periods of 10's to 100's ka (Claiborne et al., 2010; Schoene et al., 2012). We may use specific trace element characteristics, such as depletions in Th/U or increases in Yb/Gd, produced by fractionation through co-precipitating accessory phases (e.g., monazite or titanite), which are characteristic of equilibrium with the last melt. When zircon crystallizes in a magma containing a certain percentage of crystals (a crystal mush), the trace elements of the U-Pb dated zircon can be used to model the chemical evolution of melts over time, employing published zircon - melt partition coefficients (Rubatto and Hermann, 2007; Blundy and Wood, 2003). The melt signal, in turn, can subsequently be used to infer the fractionation path of the co-precipitating paragenesis during solidification, and infer the proportion of crystallized material in the magma at any time. Petrological models for melt evolution and emplacement sequence can therefore be tested quantitatively. Timescales of crystallisation and fractionation have been established for the evolution of the Fish Canyon Tuff magma by using this approach, demonstrating that the assemblage containing 0.4 vol-% titanite formed over ~ 250 ka, starting at ~28.6 Ma when

zircon saturation was reached in a magma with 40% crystals, reaching a near-solidus state at 28.4 Ma with 76% crystals, followed by thermal rejuvenation and remelting over 170 ka, and ultimately eruption at 28.2 Ma when the magma contained ~45% crystals (Wotzlaw et al., 2013; Fig. 12). The curved trend in Fig. 12 is therefore not equivalent to a liquid line of descent, but consists of thermal prograde and retrograde paths acquired during the history of the Fish Canyon Tuff magma system. Zircon thus reflects repeated re-dissolution and re-precipitation during thermal cycling of a periodically recharged magmatic system, with most of the grains recording an age of 28.4 Ma, i.e., 200 ka before eruption. The isotopic and elemental budget of a whole zircon grain is dominated by the outer growth zones because of volume considerations; the whole grain isotopic and trace element information can therefore be considered to closely approximate equilibrium with the last melt batches. Recharge can also produce a late generation of zircon which can have the opposite characteristics to earlier zircon crystallized from more evolved melts (e.g., Rivera et al., 2013).

Insert here Fig. 12

Geochronological studies should evolve to increasingly include the collection of trace element and isotope (Hf and O) data in addition to U-(Th)-Pb. This can be achieved in a number of ways. ID-TIMS analysis of whole zircons or fragments historically discarded the material separated during ion chromatographic purification which contains many petrologically useful minor and trace elements. These solutions are now commonly retained for Hf isotope (Davis et al., 2005) and trace element (Schoene et al., 2012) analysis, the latter reference coining the term 'TIMS-TEA'. This approach benefits from the fact that all data are representative of the same dissolved volume and goes some way to off-setting the problems of 'bulk' sampling for TIMS analysis when considering spatial variation within the sample material. Alternatively, high spatial resolution methods can be used to provide all of this information (albeit at lower precision) with the added benefit of spatially controlled sampling. Laser ablation-ICP-MS and SIMS techniques are complimentary in this approach and should therefore be used depending on the number of information sets required, the available volume of material and/or the volume within which analyses need to be constrained. To this end, O and Hf isotopes provide important crustal generation indicators and are determined by SIMS and LA-ICP-MS respectively. Either method can also determine the U-Pb and trace element data, so spatial resolution considerations should determine which technique is used. In order to maximize the amount of information obtained from a zircon whilst consuming the minimum amount of material, O isotope, U-Pb and trace element data

should preferentially be gathered by SIMS with Hf isotopes afterwards by LA-ICP-MS. With a moderate sacrifice in volume, the U-Pb and trace element data can also be determined by LA-ICP-MS. Increasingly, a ‘split-stream’ approach (Spencer et al., 2013, Kylander-Clark et al., 2013, Cottle et al., 2012) is being preferred for LA-ICP-MS analyses where the sample stream from one laser is split between two mass spectrometers to determine the Hf isotopes (or Nd isotopes in monazite, Goudie et al., 2014) and U-Pb or trace elements on exactly the same ablated volume. Used carefully this can help to reduce the total volume utilized whilst obtaining the maximum amount of information from a limited amount of sample material. However, the comparison of time-resolved data between the two mass spectrometers can be complicated by slight differences in instrumental set-up (e.g. tube lengths, connections, differential volumes and integration times) sometimes making the interpretation of data within an analysis difficult. In addition, if the total volume ablated for the split stream approach is greater than that required for the acquisition of one of the information sets alone, the benefit of the approach is lessened.

For isotopically uniform or structurally simple crystals, the ultimate approach is to determine the required elemental and isotopic data set by high-spatial resolution methods whilst subsequently analyzing the smallest possible portion of the crystal to obtain a high-precision U-Pb age (Rivera et al., 2014), preferably then comparing the Hf and trace elements from the wash with those data determined by high-spatial resolution (Broderick, 2013). By combining data sets from different techniques and analytical approaches, well-constrained, accurate geochronological interpretations can be made and geological interpretations greatly improved and substantiated.

Although zircon provides the most precise U-Pb data (see section 3.6) its extremely sluggish diffusion precludes the extraction of meaningful cooling rates and insights into lower temperature processes, unless (U-Th)/He data are acquired for these purposes. However, the combination of zircon with chronometers of lower retentivity (e.g., apatite, rutile, or titanite) to define P-T-t paths and fluid histories (e.g., Parrish et al., 2006; Rubatto, 2002) is a powerful tool to more completely understand tectonic and hydrothermal histories.

5. Summary and forward look

We have undoubtedly entered a new era for U-Th-Pb geochronology. Unprecedented levels of precision, spatial resolution, flexibility of approach and range of application are now

possible at increasingly higher analytical efficiency, and access to this capability for geoscientists is ever increasing. It might be asked “What is the best method or approach for U-Th-Pb dating?” Increasingly, the answer is “the one with appropriate precision and spatial resolution to answer your scientific questions appropriately, that can be demonstrated to work by validation and can be best tied most directly to other information sets”. Most likely this will mean using capabilities not available in your laboratory! Whichever single or combined approach is selected, TIMS, SIMS or LA-ICP-MS, it is important to comprehend the limitations of the techniques, not to over-interpret the data and to quantify the uncertainties correctly. The relevant questions must be asked at the beginning of a project and the analytical techniques and approaches chosen with consideration. For timescale research, highest precision and accuracy is required; this can only be provided by CA-ID-TIMS using EARTHTIME calibrated isotopic tracers and careful statistical data treatment (Schoene et al., 2006, 2013; Bowring et al., 2005; Bowring et al., 2011; McLean et al., 2011b). CA-ID-TIMS is also required to resolve comparatively ancient (>0.5 Ma) magmatic emplacement pulses (Schoene et al., 2012; Broderick, 2013) but for late Pleistocene to recent systems (<0.3 Ma) only U-Th SIMS (e.g., Claiborne et al., 2011; Schmitt, 2011), and more recently LA-ICP-MS (Bernal et al., 2014) analysis can provide the necessary temporal and spatial resolution. For the lowest volume analysis of the most precious materials (e.g. lunar accessory minerals; Grange et al., 2013; Rasmussen et al., 2011) and minerals with fine scale growth domains, SIMS is the method of choice, as well as for highest-resolution isotopic mapping and depth profiling. For the efficient accumulation of large data sets at a ± 1 -2% level of uncertainty and deeper depth profiling, LA-ICP-MS U-Pb dating is superior, and has to a great extent become the method of choice for detrital provenance and reconnaissance studies. There is still a large gap in the study of complex, ancient zircons (as, e.g., in Phanerozoic metamorphic complexes), where we need high spatial resolution for dating, analysis of other isotope systems and trace elements, but also would need high precision to decipher the sequence of metamorphic reactions.

In this new era we should discourage acceptance and publication of studies employing analytical techniques with uncertainties greater than the duration of processes required to be resolved. Averaging large numbers of low-precision analyses has repeatedly been demonstrated to produce rather precise but inaccurate average age information. Equally, in some circumstances, the true duration of events might not be determined (due to bulk

averaging), until lower precision, higher spatial resolution methods have been employed. The right tool for the job in hand must therefore be employed.

The geochronology community has taken great strides and expended much effort to understand its data quality better and how it should best be represented, as for instance in the frame of the EARTHTIME and LA-ICP-MS U-Th-Pb Network efforts. It is no longer acceptable to submit manuscripts that do not characterize the different uncertainty levels, differentiate random and systematic uncertainties, report acquisition and data handling parameters appropriately or do not give any proof of accuracy and laboratory reproducibility by presenting results for internationally validated reference materials. Reviewers should insist on these information sets and editors should refuse to accept manuscripts for review or publication without them. The reason for this is simple: interpretations and models - often considered to be the most important part of a manuscript - may be subject to change of paradigms, whilst high-quality data remain. Any geochronologic study can only persist, if data are established using state of the art technology, are supported by the most comprehensive sample characterization possible, and are well documented.

Acknowledgements

The authors are grateful for the invitation to write this review, and for careful handling by associate editor Klaus Mezger and technical editor T. Horscroft. The manuscript was greatly improved by thoughtful comments from the two journal reviewers George Gehrels and Randall R. Parrish. We acknowledge long-standing financial support by our national funding organisations (Swiss National Science Foundation, US National Science Foundation, and Natural Environment Research Council).

References:

- Allen, C.M., Campbell, I.H., 2012. Identification and elimination of a matrix-induced systematic error in LA-ICP-MS $^{206}\text{Pb}/^{238}\text{U}$ dating of zircon. *Chem. Geol.* 332–333, 157–165.
- Amelin, Y., Davies, D.W., Davies, W.J., 2005. Decoupled fractionation of even- and odd-mass isotopes of Pb in TIMS. *Geochim. Cosmochim. Acta* 69, A215
- Anderson, T. 2002. Correction of common-Pb in U-Pb analyses that do not report ^{204}Pb . *Chem. Geol.* 192, 59–79.

- Ault, A.K., Flowers, R.M., Mahan, K.H., 2012. Quartz shielding of sub-10 μm zircons from radiation damage-enhanced Pb loss: An example from a metamorphosed mafic dike, northwestern Wyoming craton. *Earth Planet. Sci. Lett.* 339-340, 57-66.
- Bachmann, O., Oberli, F., Dungan, M., Meier, M., Mundil, R., Fischer, H., 2007. $^{40}\text{Ar}/^{39}\text{Ar}$ and U–Pb dating of the Fish Canyon magmatic system, San Juan Volcanic field, Colorado: evidence for an extended crystallization history. *Chem. Geol.* 236, 134–166.
- Baldwin, S.L., Ireland, T.R., 1995. A tale of two eras: Pliocene-Pleistocene unroofing of Cenozoic and late Archean zircons from active metamorphic core complexes, Solomon Sea, Papua New Guinea. *Geology* 23, 1023-1026.
- Bernal, J.P., Solari, L.A., Gómez-Tuena, A., Ortega-Obregón, C., Mori, L., Vega-González, M., Espinosa-Arbeláez, D.G., 2014. In-situ $^{230}\text{Th}/\text{U}$ dating of Quaternary zircons using LA-MC ICP MS. *Quat. Geochron.* 23, 46-55.
- Black, L.P., Gulson, B.L., 1978. The age of the Mud Tank carbonatite, Strangeways Range, Northern Territory. *BMR J. Austr. Geol. Geophys.* 3, 227–232.
- Black, L.P., Kamo, S.L., Allen, C.M., Aleinikoff, J.N., Davis, D.W., Korsch, R.J., Foudoulis, C., 2003. TEMORA 1: a new zircon standard for Phanerozoic U–Pb geochronology. *Chem. Geol.* 200, 155–170.
- Black, L.P., Kamo, S.L., Allen, C.M., Davis, D.W., Aleinikoff, J.N., Valley, J.W., Mundil, R., Campbell, I.H., Korsch, R.J., Williams, I.S., Foudoulis C., 2004. Improved $^{206}\text{Pb}/^{238}\text{U}$ microprobe geochronology by the monitoring of a trace-element-related matrix effect; SHRIMP, ID–TIMS, ELA–ICP–MS and oxygen isotope documentation for a series of zircon standards. *Chem. Geol.* 205, 115–140.
- Blundy, J., Wood, B., 2003. Partitioning of trace elements between crystals and melts. *Earth Planet. Sci. Lett.* 210, 383–397.
- Boehnke, P., Harrison, T.M., 2014. A meta-analysis of geochronologically relevant half-lives: what’s the best decay constant?. *Int. Geol. Rev.* 56, 905-914.
- Boehnke, P., Watson, E.B., Trail, D., Harrison, T. M., Schmitt, A.K. (2013). *Chem. Geol.* 351, 324–334.
- Boekhout, F., Spikings, R., Sempere, T., Chiaradia, M., Ulianov, A., Schaltegger, U., 2012. Mesozoic arc magmatism along the southern Peruvian margin during Gondwana breakup and dispersal. *Lithos* 146-147, 48–64.
- Bosse, V., Boulvais, P., Gautier, P., Tiepolo, M., Ruffet, G., Devidal, J. L., Cherneva, Z., Gerjikov, I., Paquette, J. L., 2009. Fluid-induced disturbance of the monazite Th–Pb chronometer: in situ dating and element mapping in pegmatites from the Rhodope (Greece, Bulgaria). *Chem. Geol.* 261, 286-302.
- Bowring, S.A., Erwin, D., Parrish, R.R., Renne, P., 2005. EARTHTIME: A community-based effort towards high-precision calibration of earth history. *Geochim. Cosmochim. Acta*, 69, A316–A316.
- Bowring, J.F., Horstwood, M.S.A., Gehrels, G., 2013. Resolving bias in laser ablation geochronology. *Eos*, Vol. 94, No. 24.
- Bowring, J.F., Mclean, N.M., Bowring, S.A., 2011. Engineering cyber infrastructure for U–Pb geochronology: Tripoli and U–Pb_Redux. *Geochem. Geophys. Geosyst.* 12, Q0AA19. doi:10.1029/2010GC003479.
- Broderick C., 2013. Timescales and petrological processes during incremental pluton assembly: a case study from the Val Fredda Complex, Adamello Batholith, N. Italy. Unpubl. Thesis no. 4612 Univ. de Genève, 169pp.

- Burnham, A.D., Berry, A.J., 2012. An experimental study of trace element partitioning between zircon and melt as a function of oxygen fugacity. *Geochimica et Cosmochimica Acta* 95, 196-212.
- Caricchi, L., Simpson, G., Schaltegger, U., 2014. Zircons reveal magma fluxes in the Earth's crust. *Nature* 511, 457-461.
- Catlos, E.J., Gilley, L.D. Harrison, T.M., 2002. Interpretation of monazite ages obtained via in situ analysis. *Chem. Geol.* 188, 193-215.
- Charlier, B.L.A., Wilson, C.J.N., 2010. Chronology and evolution of caldera-forming and post-caldera magma systems at Okataina Volcano, New Zealand from zircon U-Th model-age spectra. *J. Petrol.* 51, 1121-1141.
- Charlier, B.L.A., Peate, D.W., Wilson, C.J.N., Lowenstern, J.B., Storey, M. Brown, S.J.A., 2003. Crystallisation ages in coeval silicic magma bodies; ^{238}U - ^{230}Th disequilibrium evidence from the Rotoiti and Earthquake Flat eruption deposits, Taupo volcanic zone, New Zealand. *Earth Planet. Sci. Lett.* 206, 441-457.
- Charlier, B.L.A., Wilson, C.J.N., Lowenstern, J.B., Blake, S., van Calsteren, P.W. Davidson, J.P., 2005. Magma generation at a large, hyperactive silicic volcano (Taupo, New Zealand) revealed by U-Th and U-Pb systematics in zircons. *J. Petrol.* 46, 3-32.
- Cheng, H., Edwards, L.R., Shen, C.C., Polyak, V.J., Asmerom, Y., Woodhead, J., Hellstrom, J., Wang, Y., Kong, X., Spötl, C., Wang, X., 2013. Improvements in ^{230}Th dating, ^{230}Th and ^{234}U half-life values, and U-Th isotopic measurements by multi-collector inductively coupled plasma mass spectrometry. *Earth and Planetary Science Letters* 371, 82-91.
- Chew, D.M., Petrus, J.A., Kamber, B.S., 2014. U-Pb LA-ICPMS dating using accessory mineral standards with variable common Pb. *Chem. Geol.* 363, 185-199.
- Chew, D. M., Sylvester, P. J., Tubrett, M. N., 2011. U-Pb and Th-Pb dating of apatite by LA-ICPMS. *Chem. Geol.* 280, 200-216.
- Chiaradia, M., Schaltegger, U., Spikings, R., 2013. How Accurately Can We Date the Duration of Magmatic-Hydrothermal Events in Porphyry Systems?—An Invited Paper. *Econ. Geol.* 108, 565-584.
- Claiborne, L.L., Miller, C.F., Flanagan, D M., Clynne, M A., Wooden, J.L., 2010. Zircon reveals protracted magma storage and recycling beneath Mount St. Helens. *Geology* 38, 1011-1014.
- Compston, W., Williams, I.S. Meyer, C.E., 1984. U-Pb geochronology of zircons from lunar breccia 73217 using a sensitive high mass-resolution ion microprobe. *J. Geophys. Res.* 89, Suppl.(B), 525-534.
- Condon, D.J., 2005. Progress report on the U-Pb interlaboratory experiment. *Geochim. Cosmochim. Acta*, Suppl., 69, 319.
- Condon, D.J., McLean, N., Noble, S.R., Bowring, S.A., 2010. Isotopic composition ($^{238}\text{U}/^{235}\text{U}$) of some commonly used uranium reference materials. *Geochim. Cosmochim. Acta* 74, 7127-7143.
- Condon, D. J., Schoene, B., McLean, N. M., Bowring, S., Parrish, R. R. Metrology and Traceability of U-Pb Isotope Dilution Geochronology (EARTHTIME Tracer Calibration Part I). *Geochim. Cosmochim. Acta*, in review.
- Cooper, K.M., Kent, A.J.R., 2014. Rapid remobilization of magmatic crystals kept in cold storage. *Nature* 506, 480-485.
- Cottle, J.M., Horstwood, M.S.A. Parrish, R.R., 2009. A new approach to single shot laser ablation analysis and its application to in situ Pb/U geochronology. *J. Anal. Atom. Spectrom.* 24, 1355-1363.

- Cottle, J.M., Kylander-Clark, A.R., Vrijmoed, J.C., 2012. U–Th/Pb geochronology of detrital zircon and monazite by single shot laser ablation inductively coupled plasma mass spectrometry (SS-LA-ICPMS). *Chem. Geol.* 332–333 (2012) 136–147.
- Crowley, J., Schoene, B., Bowring, S., 2007. U–Pb dating of zircon in the Bishop Tuff at the millennial scale. *Geology* 35, 1123.
- Crowley, Q.G., Heron, K., Riggs, N., Kamber, B., Chew, D., McConnell, B., Benn, K., 2014. Chemical Abrasion Applied to LA-ICP-MS U–Pb Zircon Geochronology. *Minerals* 4, 503–518.
- D'Abzac, F.-X., Seydoux-Guillaume, A.-M., Chmeleff, J., Datas, L., Poitrasson, F., 2011. Study of near infra red femtosecond laser induced particles using transmission electron microscopy and low pressure impaction: Implications for laser ablation–inductively coupled plasma-mass spectrometry analysis of natural monazite, *Spectrochim. Acta Part B: Atomic Spectroscopy*, 66, 671–680.
- Danišik, M., Shane, P., Schmitt, A.K., Hogg, A., Santos, G.M., Storm, S., Evans, N., Fifield, K., Lindsay, J.M., 2012. Re-anchoring the late Pleistocene tephrochronology of New Zealand based on concordant radiocarbon ages and combined $^{238}\text{U}/^{230}\text{Th}$ disequilibrium and (U–Th)/He zircon ages. *Earth and Planetary Science Letters* 349, 240–250.
- Dalrymple, G.B., Grove, M., Lovera, O.M., Harrison, T.M., Hulen, J.B., Lanphere, M.A., 1999. Age and thermal history of the Geysers plutonic complex (felsite unit), Geysers geothermal field, California: a $^{40}\text{Ar}/^{39}\text{Ar}$ and U–Pb study. *Earth and Planetary Science Letters* 173(3), 285–298.
- Davis, D.W., Amelin, Y., Nowell, G.M., Parrish, R.R., 2005. Hf isotopes in zircon from the western Superior province, Canada: Implications for Archean crustal development and evolution of the depleted mantle reservoir. *Precambrian Res.* 140, 132–156.
- Dickinson, W.R., Gehrels, G.E., 2009. Use of U–Pb ages of detrital zircons to infer maximum depositional ages of strata: A test against a Colorado Plateau Mesozoic database. *Earth Planet. Sci. Lett.* 288, 115–125.
- Dobrzhinetskaya, L., Wirth, R., Green, H., 2014. Diamonds in Earth's oldest zircons from Jack Hills conglomerate, Australia, are contamination. *Earth Planet. Sci. Lett.* 387, 212–218.
- Feng, R., Machado, N. Ludden, J., 1993. Lead geochronology of zircon by laserprobe-inductively coupled plasma mass spectrometry (LP-ICPMS). *Geochim. Cosmochim. Acta* 57, 3479–3486.
- Fletcher, I.R., McNaughton, N.J., Davis, W.J. Rasmussen, B., 2010. Matrix effects and calibration limitations in ion probe U/Pb and Th/Pb dating of monazite. *Chem. Geol.* 270, 31–44.
- Foster, G., Parrish, R.R., Horstwood, M.S., Chenery, S., Pyle, J., Gibson, H.D., 2004. The generation of prograde P–T–t points and paths; a textural, compositional, and chronological study of metamorphic monazite. *Earth and Planetary Science Letters* 228(1), 125–142.
- Frei, D., Gerdes, A., 2009. Precise and accurate in situ U–Pb dating of zircon with high sample throughput by automated LA-SF-ICP-MS. *Chem. Geol.* 261, 261–270.
- Fryer, B.J., Jackson, S.E. Longerich, H.P., 1993. The application of laser ablation microprobe-inductively coupled plasma-mass spectrometry (LAM-ICP-MS) to in situ (U)–Pb geochronology. *Chem. Geol.* 109, 1–8.
- Gehrels, G.E., Valencia, V.A. Ruiz, J., 2008. Enhanced precision, accuracy, efficiency, and spatial resolution of U–Pb ages by laser ablation–multicollector–inductively coupled plasma-mass spectrometry, *Geochem. Geophys. Geosyst.* 9, Q03017, doi:10.1029/2007GC001805.

- Gerdes, A., Zeh, A., 2009. Zircon formation versus zircon alteration—new insights from combined U–Pb and Lu–Hf in-situ LA-ICP-MS analyses, and consequences for the interpretation of Archean zircon from the Central Zone of the Limpopo Belt. *Chem. Geol.* 261, 230-243.
- Gerstenberger, H., Haase, G., 1997. A highly effective emitter substance for mass spectrometric Pb isotope ratio determinations. *Chem. Geol.* 136, 309–312.
- Goudie, D.J., Fisher, C.M., Hanchar, J.M., Crowley, J.L. Ayers, J.C., 2014. Simultaneous in situ determination of U-Pb and Sm-Nd isotopes in monazite by laser ablation ICP-MS. *Geochem. Geophys. Geosyst.* 15, 2575-2600, doi:10.1002/2014GC005431.
- Grange, M.L., Pidgeon, R.T., Nemchin, A.A., Timms, N.E., Meyer, C., 2013. Interpreting U–Pb data from primary and secondary features in lunar zircon. *Geochim. Cosmochim. Acta* 101, 112–132.
- Guex, J., Schoene, B., Bartolini, A., Spangenberg, J., Schaltegger, U., O'Dogherty, L., Taylor, D., Bucher, H., Atudorei, V., 2012. Geochronological constraints on post-extinction recovery of the ammonoids and carbon cycle perturbations during the Early Jurassic. *Palaeogeogr. Palaeoclimat. Palaeoecol.* 346-347, 1–11.
- Guillong, M., Horn, I., Günther, D. 2003. A comparison of 266nm, 213nm and 193nm produced from a single solid state Nd:YAG laser for laser ablation ICP-MS. *J. Anal. At. Spectrom.*, 18, 1224-1230.
- Hanchar, J.M., 2009. Results from a round-robin study assessing the precision and accuracy of LA-ICPMS U/Pb geochronology of zircon. *Eos Trans. AGU*, 90, Fall Meet. Suppl., Abs.: V53B-04
- Harrison, T.M., McKeegan, K.D., LeFort, P. 1995 Detection of inherited monazite in the Manaslu leucogranite by $^{208}\text{Pb}/^{232}\text{Th}$ ion microprobe dating: Crystallization age and tectonic implications. *Earth Planet. Sci. Letts.*, 133, Issues 3–4, 271–282.
- Harrison, T.M., Schmitt, A.K., 2007. High sensitivity mapping of Ti distributions in Hadean zircons. *Earth Planet. Sci. Lett.* 261, 9-19.
- Hellebrand, E., Moeller, A., Whitehouse, M. Cannat, M., 2007. Formation of oceanic zircons. *Geochim. Cosmochim. Acta* 71, A391.
- Hietpas, J., Samson, S., Moecher, D. Schmitt, A.K., 2010. Recovering tectonic events from the sedimentary record; detrital monazite plays in high fidelity. *Geology* 38, 167-170.
- Hiess, J., Condon, D. J., McLean, N., Noble, S. R., 2012. $^{238}\text{U}/^{235}\text{U}$ Systematics in Terrestrial Uranium-Bearing Minerals. *Science* 335, 1610–1610.
- Hofmann, A.E., Valley, J.W., Watson, E.B., Cavosie, A.J. Eiler, J.M., 2009. Sub-micron scale distributions of trace elements in zircon. *Contrib. Mineral. Petrol.* 158, 317-335.
- Holden, P., Lanc, P., Ireland, T. R., Harrison, T. M., Foster, J. J., Bruce, Z., 2009. Mass-spectrometric mining of Hadean zircons by automated SHRIMP multi-collector and single-collector U/Pb zircon age dating: The first 100,000 grains. *International Journal of Mass Spectrometry*, 286(2), 53-63.
- Horn, I., von Blanckenburg, F. 2007. Investigation on elemental and isotopic fractionation during 196 nm femtosecond laser ablation multiple collector inductively coupled plasma mass spectrometry. *Spectrochim. Acta B*, 62, issue 4, 410-422.
- Hunter, J.L., 2009. Improving Depth Profile Measurements of Natural Materials: Lessons Learned from Electronic Materials Depth-Profiling, in: Fayek, M. (Ed.), *Secondary Ion Mass Spectrometry in the Earth Sciences: Gleaning the Big Picture from a Small Spot*. Short Course Series. Mineral. Assoc. Canada (MAC), Québec, 133-148.

- Huyskens, M. H., Iizuka, T., Amelin, Y., 2012. Evaluation of colloidal silicagels for lead isotopic measurements using thermal ionisation mass spectrometry. *J. Anal. Atom. Spectrom.* 27, 1439-1446.
- Ickert, R.B., Hiess, J., Williams, I.S., Holden, P., Ireland, T.R., Lanc, P., Schram, N., Foster, J.J. Clement, S.W., 2008. Determining high precision, in situ, oxygen isotope ratios with a SHRIMP II; analyses of MPI-DING silicate-glass reference materials and zircon from contrasting granites. *Chem. Geol.* 257, 114-128.
- Ireland, T.R., Williams, I.S., 2003. Considerations in zircon geochronology by SIMS. *Rev. Mineral. Geochem.* 53, 215-241.
- Jackson, S., Pearson, N., Griffin, W., Belousova, E., 2004. The application of laser ablation-inductively coupled plasma-mass spectrometry to in situ U–Pb zircon geochronology. *Chem. Geol.* 211, 47–69.
- Janots, E., Berger, A., Gnos, E., Whitehouse, M., Lewin, E., Pettke, T., 2012. Constraints on fluid evolution during metamorphism from U–Th–Pb systematics in Alpine hydrothermal monazite. *Chem. Geol.* 326, 61-71.
- Jeon, H., Whitehouse, M. J. (2014). A Critical Evaluation of U–Pb Calibration Schemes Used in SIMS Zircon Geochronology. *Geostandards and Geoanalytical Research*. DOI: 10.1111/j.1751-908X.2014.00325.x
- Johnston, S., Gehrels, G., Valencia, V., Ruiz, J., 2009. Small volume U–Pb zircon geochronology by laser ablation-multicollector-ICP-MS. *Chem. Geol.* 259, 218–229.
- Kalsbeek, F., 1992. The statistical distribution of the mean squared weighted deviation—comment: Isochrons, errorchrons, and the use of MSWD-values. *Chem. Geol.* 94, 241-242.
- Kennedy A.K., Wotzlaw J.F., Crowley J., Schmitz M. Schaltegger U., 2014. Eocene reference material for microanalysis of U–Th–Pb isotopes and trace elements. *Can. Mineral.* 52, in press.
- Klemetti, E.W., Deering, C.D., Cooper, K.M. Roeske, S.M., 2011. Magmatic perturbations in the Okataina Volcanic Complex, New Zealand at thousand-year timescales recorded in single zircon crystals. *Earth Planet. Sci. Lett.* 305, 185-194.
- Koch, J., Wälle, M., Pisonero, J., Günther, D., 2006. Performance characteristics of ultra-violet femtosecond laser ablation inductively coupled plasma mass spectrometry at ~265 and ~200 nm. *J. Analyt. Atom. Spectrom.* 21, 932-940.
- Koch, J., Günther, D., 2011. Review of the state-of-the-art of laser ablation inductively coupled plasma mass spectrometry. *Appl. Spectroscopy* 65, 155A-162A.
- Kooijman, E., Mezger, K., Berndt, J., 2010. Constraints on the U–Pb systematics of metamorphic rutile from in-situ LA-ICP-MS analysis. *Earth Planet. Sci Letts*, 293, 321-330
- Kooijman, E., Berndt, J., Mezger, K., 2012. U–Pb dating of zircon by laser ablation ICP-MS: recent improvements and new insights. *European J. Mineral.* 24, 5-21.
- Koornneef, J.M., Dorta, L., Hattendorf, B., Fontaine, G.H., Bourdon, B., Stracke, A., Ulmer, P., Günther D., 2012. *In situ* analysis of ^{230}Th – ^{232}Th – ^{238}U ratios in titanite by fs-LA-MC-ICPMS. *J. Anal. At. Spectrom.* 27, 1863-1874.
- Košler, J., Tubrett, M.N., Sylvester, P.J., 2001. Application of Laser Ablation ICP-MS to U–Th–Pb Dating of Monazite. *Geostand. Newsletters* 25, 375-386.
- Košler, J., Sláma, J., Belousova, E., Corfu, F., Gehrels, G. E., Gerdes, A., Horstwood, M.S.A., Sircombe, K.N., Sylvester, P.J., Tiepolo, M., Whitehouse, M.J., Woodhead, J.D., 2013. U–Pb detrital zircon analysis - results of an inter-laboratory comparison. *Geostand. Geoanal. Res.* 37, 243–259.

- Krogh, T.E., 1982. Improved accuracy of U–Pb zircon ages by the creation of more concordant systems using an air abrasion technique. *Geochim. Cosmochim. Acta* 46, 637–649.
- Kryza, R., Crowley, Q.G., Larionov, A., Pin, C., Oberc-Dziedzic, T. Mochnacka, K., 2012. Chemical abrasion applied to SHRIMP zircon geochronology: An example from the Variscan Karkonosze Granite (Sudetes, SW Poland). *Gondwana Res.* 21, 757–767.
- Kusiak, M.A., Whitehouse, M.J., Wilde, S.A., Nemchin, A.A., Clark, C., 2013. Mobilization of radiogenic Pb in zircon revealed by ion imaging: Implications for early Earth geochronology. *Geology* 41, 291–294.
- Kylander-Clark, A.R.C., Hacker, B.R., Cottle, J.M., 2013. Laser-ablation split-stream ICP petrochronology, *Chem. Geol.* 345, Pages 99–112
- Li, Q.L., Li, X.H., Liu, Y., Tang, G.Q., Yang, J.H., Zhu, W.G., 2010. Precise U–Pb and Pb–Pb dating of Phanerozoic baddeleyite by SIMS with oxygen flooding technique. *J. Anal. Atom. Spectrom.* 25, 1107–1113.
- Ludwig, K.R., 2003. Isoplot 3.00 A Geochronological toolkit for Microsoft Excel. Berkeley Geochron. Center Spec. Publ. 4, 71 pp.
- Machado, N., Gauthier, G., 1996. Determination of $^{207}\text{Pb}/^{206}\text{Pb}$ ages on zircon and monazite by laser-ablation ICPMS and application to a study of sedimentary provenance and metamorphism in southeastern Brazil. *Geochim. Cosmochim. Acta*, 60, 5063–5073.
- Mahon, K.I., 1996. The New “York” regression: Application of an improved statistical method to geochemistry. *International Geology Review* 38(4), 293–303.
- Marillo-Sialer, E., Woodhead, J., Hergt, J., Greig, A., Guillong, M., Gleadow, A., Evans., N., Paton, C., 2014. The zircon ‘matrix effect’: evidence for an ablation rate control on the accuracy of U–Pb age determinations by LA-ICP-MS. *J. Anal. At. Spectrom.* 29, 981–989.
- Mattinson, J., 2005. Zircon U–Pb chemical abrasion (“CA-TIMS”) method: combined annealing and multi-step partial dissolution analysis for improved precision and accuracy of zircon ages. *Chem. Geol.* 220, 47–66.
- Mattinson, J.M., 2010. Analysis of the relative decay constants of ^{235}U and ^{238}U by multi-step CA-TIMS measurements of closed-system natural zircon samples. *Chem. Geol.* 275, 186–198.
- Mays, C.W., Atherton, D.R., Lloyd, R.D., Lucas, H.F., Stover, B.J., Bruenger, F.W., 1962. The half-period of Ra 228 (Mesothorium)”, Utah Univ. Report, COO-225, 92–105.
- McLean, N.M., Amelin Y.V., Bowring, S.A., 2011a. Quantification of mass independent fractionation in Pb by TIMS and implications for U–Pb geochronology. Abstract V33G-05, Fall Meeting, AGU, San Francisco, Calif., 5–9 Dec. 2011.
- McLean, N.M., Bowring, J.F., Bowring, S.A., 2011b. An algorithm for U–Pb isotope dilution data reduction and uncertainty propagation. *Geochem. Geophys. Geosyst.* 12, Q0AA18. doi:10.1029/2010GC003478
- Miller, J., Matzel, J., Miller, C., Burgess, S., Miller, R., 2007. Zircon growth and recycling during the assembly of large, composite arc plutons. *J. Volcanol. Geotherm. Res.* 167, 282–299.
- Möller, A., O’Brien, P.J., Kennedy, A. Kröner, A., 2003. Linking growth episodes of zircon and metamorphic textures to zircon chemistry; an example from the ultrahigh-temperature granulites of Rogaland, SW Norway. *Geol. Soc. London, Spec. Publ.* 220, 65–81.
- Moser, D.E., Davis, W.J., Reddy, S.M., Flemming, R.L. Hart, R.J., 2009. Zircon U–Pb strain chronometry reveals deep impact-triggered flow. *Earth Planet. Sci. Lett.* 277, 73–79.

- Müller, W., Shelley, M., Miller, P., Broude, S., 2009. Initial performance metrics of a new custom-designed ArF excimer LA-ICPMS system coupled to a two-volume laser-ablation cell. *J. Analyt. Atom. Spectrom.* 24, 209-214.
- Murray, K.K., Boyd, R.K., Eberlin, M.N., Langley, G.J., Li, L. and Naito, T. 2013. Definition of terms relating to mass spectrometry (IUPAC recommendations 2013). *Pure Appl. Chem.*, 85, 1515-1609.
- Paces, J. B., Miller, J. D., 1993. Precise U-Pb Ages of Duluth Complex and Related Mafic Intrusions, Northeastern Minnesota - Geochronological Insights to Physical, Petrogenetic, Paleomagnetic, and Tectonomagmatic Processes Associated with the 1.1 Ga Midcontinent Rift System. *J. Geophys. Res.* 98(B8), 13997–14013.
- Palacz, Z., Jones, T., Tootel, D., Guest, R., Locke, S., 2011. Performance characteristics of an enhanced Daly ion counting system for TIMS. *Min. Mag.* 75, 1588.
- Parrish, R.R., Noble, S., 2003. Zircon U-Th-Pb geochronology by isotope dilution - thermal ionization mass spectrometry (ID-TIMS), in: Hanchar, J.M., Koskin, P.O.W. (eds.) *Zircon. Rev. Mineral. Geochem.* 53, 183-213.
- Parrish, R.R., Gough, S.J., Searle, M.P., Waters, D.J., 2006. Plate velocity exhumation of ultrahigh-pressure eclogites in the Pakistan Himalaya. *Geology*, 34, 989-992.
- Peres, P., Kita, N.T., Valley, J.W., Fernandes, F. and Schuhmacher, M., 2012. New sample holder geometry for high precision isotope analyses. *Surface and Interface Analysis* 45(1), 553-556.
- Peterman E.M., Mattinson, J.M. Hacker B.R. 2012. Multi-step TIMS and CA-TIMS monazite U-Pb geochronology. *Chem. Geol.* 312-313, 58–73.
- Pullen, A., Ibáñez-Mejía, M., Gehrels, G.E., Ibáñez-Mejía, J.C., Pecha, M., 2014. What happens when n= 1000? Creating large-n geochronological datasets with LA-ICP-MS for geologic investigations. *J. Anal. At. Spectrom.*, 2014,29, 971-980
- von Quadt, A., Gallhofer, D., Guillong, M., Peytcheva, I., Waelle, M., Sakata, S., 2014. U-Pb dating of CA/non-CA treated zircons obtained by LA-ICP-MS and CA-TIMS techniques: impact for their geological interpretation. *J. Anal. At. Spectrom.* 29, 1618-1629.
- Rasmussen, B., 2005. Zircon growth in very low grade metasedimentary rocks: evidence for zirconium mobility at ~ 250 C. *Contrib. Mineral. Petrol.* 150(2), 146-155.
- Rasmussen, B., Fletcher, I. R., Gregory, C. J., Muhling, J. R., Suvorova, A. A., 2011. Tranquillityite: The last lunar mineral comes down to Earth. *Geology* 40, 83–86.
- Reid, M.R., Coath, C.D., Harrison, T.M. McKeegan, K.D., 1997. Prolonged residence times for the youngest rhyolites associated with Long Valley Caldera; ²³⁰Th-²³⁸U ion microprobe dating of young zircons. *Earth Planet. Sci. Lett.* 150, 27-39.
- Reid, M.R., Vazquez, J.A., Schmitt, A.K., 2011. Zircon-scale insights into the history of a Supervolcano, Bishop Tuff, Long Valley, California, with implications for the Ti-in-zircon geothermometer. *Contributions to Mineralogy and Petrology* 161(2), 293-311.
- Renne, P.R., Mundil, R., Balco, G., Min, K., Ludwig, K.R., 2010. Joint determination of 40K decay constants and 40Ar/40K for the Fish Canyon sanidine standard, and improved accuracy for 40Ar/39Ar geochronology. *Geochim. Cosmochim. Acta* 74, 5349–5367.

- Richter, S., Goldberg, S., Mason, P., Traina, A., Schwieters, J., 2001. Linearity tests for secondary electron multipliers used in isotope ratio mass spectrometry. *Int. J. Mass Spectrom.* 206, 105–127.
- Rioux, M., Bowring, S., Dudás, F., Hanson, R., 2010. Characterizing the U–Pb systematics of baddeleyite through chemical abrasion: application of multi-step digestion methods to baddeleyite geochronology. *Contrib. Mineral. Petrol.* 160, 777–801.
- Rioux, M., Lissenberg, C. J., McLean, N. M., Bowring, S. A., MacLeod, C. J., Hellebrand, E., Shimizu, N., 2012. Protracted timescales of lower crustal growth at the fast-spreading East Pacific Rise. *Nature Geosci.* 5, 275–278.
- Rivera, T.A., Schmitz, M.D., Crowley J.L., Storey, M., 2014. Rapid magma evolution constrained by zircon petrochronology and $^{40}\text{Ar}/^{39}\text{Ar}$ sanidine ages for the Huckleberry Ridge Tuff, Yellowstone, USA. *Geology* 42, 643–646.
- Rivera, T.A., Storey, M., Schmitz, M.D., Crowley, J.L., 2013. Age intercalibration of $^{40}\text{Ar}/^{39}\text{Ar}$ sanidine and chemically distinct U/Pb zircon populations from the Alder Creek Rhyolite Quaternary geochronology standard. *Chemical Geology* 345, 87–98.
- Robert, J., Miranda, C.F., Muxart, R., 1969. Mesure de la période du protactinium 231 par microcalorimétrie. *Radiochimica Acta* 11(2), 104–108.
- Romer, R.L., 2003. Alpha-recoil in U–Pb geochronology: effective sample size matters. *Contributions to Mineralogy and Petrology* 145(4), 481–491.
- Rubatto, D., 2002. Zircon trace element geochemistry: partitioning with garnet and the link between U–Pb ages and metamorphism. *Chem. Geol.* 184, 123–138.
- Rubatto, D., Hermann, J., 2007. Experimental zircon/melt and zircon/garnet trace element partitioning and implications for the geochronology of crustal rocks. *Chem. Geol.* 241, 38–61.
- Russo, R. E., Mao, X., Gonzalez, J. J., Zorba, V., Yoo, J., 2013. Laser ablation in analytical chemistry. *Analyt. Chem.* 85, 6162–6177.
- Sanudo-Wilhelmy, S.A., Flegal, A.R., 1994. Temporal Variations in Lead Concentrations and Isotopic Composition in the Southern California Bight. *Geochim. Cosmochim. Acta* 58, 3315–3320.
- Schärer, U., 1984. The effect of initial ^{230}Th disequilibrium on young U–Pb ages; the Makalu case, Himalaya. *Earth Planet. Sci. Lett.* 67, 191–204.
- Schaltegger, U., Brack, P., Ovtcharova, M., Peytcheva, I., Schoene, B., Stracke, A., Marocchi, M., Bargossi, G.M., 2009. Zircon and titanite recording 1.5 million years of magma accretion, crystallization and initial cooling in a composite pluton (southern Adamello batholith, northern Italy). *Earth Planet. Sci. Lett.* 286, 208–218.
- Schmitt, A. K., 2011. Uranium Series Accessory Crystal Dating of Magmatic Processes. *Ann. Rev. Earth Planet. Sci.* 39, 321–349.
- Schmitt, A.K., Zack, T., 2012. High-sensitivity U–Pb rutile dating by secondary ion mass spectrometry (SIMS) with an O_2^+ primary beam. *Chemical Geology* 332, 65–73.
- Schmitt, A.K., Chamberlain, K.R., Swapp, S.M., Harrison, T.M., 2010. In situ U–Pb dating of micro-baddeleyite by secondary ion mass spectrometry. *Chemical Geology* 269(3), 386–395.

- Schmitz, M., Bowring, S., 2001. U-Pb zircon and titanite systematics of the Fish Canyon Tuff: an assessment of high-precision U-Pb geochronology and its application to young volcanic rocks. *Geochim. Cosmochim. Acta* 65, 2571–2587.
- Schoene, B., 2014. U–Th–Pb Geochronology. *The Crust* (2nd ed., Vol. 4, pp. 341–378). Elsevier Ltd.
- Schoene, B., Condon, D.J., Morgan, L., McLean, N., 2013. Precision and accuracy in Geochronology. *Elements* 9, 19–24.
- Schoene, B., Crowley, J., Condon, D., Schmitz, M., Bowring, S., 2006. Reassessing the uranium decay constants for geochronology using ID-TIMS U–Pb data. *Geochim. Cosmochim. Acta* 70, 426–445.
- Schoene, B., Guex, J., Bartolini, A., Schaltegger, U., Blackburn, T. J., 2010a. Correlating the end-Triassic mass extinction and flood basalt volcanism at the 100 ka level. *Geology* 38, 387–390.
- Schoene, B., Latkoczy, C., Schaltegger, U., Günther, D., 2010b. A new method integrating high-precision U–Pb geochronology with zircon trace element analysis (U–Pb TIMS-TEA). *Geochim. Cosmochim. Acta* 74, 7144–7159.
- Schoene, B., Schaltegger, U., Brack, P., Latkoczy, C., Stracke, A., Günther, D., 2012. Rates of magma differentiation and emplacement in a ballooning pluton recorded by U–Pb TIMS-TEA, Adamello batholith, Italy. *Earth Planet. Sci. Lett.* 355–356, 162–173.
- Schumacher, M., De Chambost, E., McKeegan, K.D., Harrison, T.M., Migeon, H., 1994. In situ dating of zircon with the CAMECA ims 1270 Secondary Ion Mass Spectrometry, in: Benninghoven, A., Werner, H.W., Shimizu, R., Nihei, Y. (eds.), *SIMS. IX*. John Wiley & Sons, pp. 919–922.
- Shaheen, M. E., Gagnon, J. E., Fryer, B. J., 2012. Femtosecond (fs) lasers coupled with modern ICP-MS instruments provide new and improved potential for in situ elemental and isotopic analyses in the geosciences. *Chem. Geol.* 330–331, 260–273.
- Shane, P., Storm, S., Schmitt, A.K., Lindsay, J.M., 2012. Timing and conditions of formation of granitoid clasts erupted in recent pyroclastic deposits from Tarawera Volcano (New Zealand). *Lithos* 140–141, 1–10.
- Simon, J.I., Reid, M.R., 2005. The pace of rhyolite differentiation and storage in an "archetypical" silicic magma system, Long Valley, California. *Earth Planet. Sci. Lett.* 235, 123–140.
- Sláma, J., Košler, J., Condon, D.J., Crowley, J.L., Gerdes, A., Hanchar J.M., Horstwood, M.S.A., Morris, G.A., Nasdala, L., Norberg, N., Schaltegger, U., Schoene, B., Tubrett, M.N., Whitehouse, M.J., 2008. Plešovice zircon – a new natural reference material for U-Pb and Hf isotopic microanalysis. *Chem. Geol.* 249, 1–35.
- Spencer, K.J., Hacker, B.R., Kylander-Clark, A.R.C., Andersen, T.B., Cottle, J.M., Stearns, M.A., Poletti, J.E., Seward, G.G.E., 2013. Campaign-style titanite U–Pb dating by laser-ablation ICP: Implications for crustal flow, phase transformations and titanite closure, *Chem. Geol.* 341, 84–101.
- Stacey, J.S., Kramers, J.D., 1975. Approximation of terrestrial lead isotope evolution by a two-stage model. *Earth Planet. Sci. Lett.* 26, 207–221.
- Steely, A.N., Hourigan, J.K., Juel, E., 2014. Discrete multi-pulse laser ablation depth profiling with a single-collector ICP-MS: Sub-micron U–Pb geochronology of zircon and the effect of radiation damage on depth-dependent fractionation, *Chem. Geol.* 372, Pages 92–108.
- Stelten, M.E., Cooper, K.M., Vazquez, J.A., Reid, M.R., Barfod, G.H., Wimpenny, J., Yin, Q.Z., 2013. Magma mixing and the generation of isotopically juvenile silicic magma at Yellowstone caldera inferred from

- coupling ^{238}U - ^{230}Th ages with trace elements and Hf and O isotopes in zircon and Pb isotopes in sanidine. *Contributions to Mineralogy and Petrology* 166(2), 587-613.
- Stern, R.A., Amelin, Y., 2003. Assessment of errors in SIMS zircon U-Pb geochronology using a natural zircon standard and NIST SRM 610 glass. *Chem. Geol.* 197, 111-142.
- Stern, R.A., Bodorkos, S., Kamo, S.L., Hickman, A.H., Corfu, F., 2009. Measurement of SIMS instrumental mass fractionation of Pb isotopes during zircon dating. *Geostand. Geoanal. Res.* 33, 145-168.
- Storey, C.D., Jeffries, T.E., Smith, M., 2006. Common lead-corrected laser ablation ICP-MS U-Pb systematics and geochronology of titanite, *Chem. Geol.* 227, 37-52.
- Storm, S., Shane, P., Schmitt, A.K., Lindsay, J.M., 2011. Contrasting punctuated zircon growth in two syn-erupted rhyolite magmas from Tarawera volcano: Insights to crystal diversity in magmatic systems. *Earth Planet. Sci. Lett.* 301, 511-520.
- Storm, S., Shane, P., Schmitt, A.K., Lindsay, J.M., 2012. Decoupled crystallization and eruption histories of the rhyolite magmatic system at Tarawera Volcano revealed by zircon ages and growth rates. *Contrib. Mineral. Petrol.* 163, 505-519.
- Storm, S., Schmitt, A.K., Shane, P., Lindsay, J.M., 2014. Zircon trace element chemistry at sub-micrometer resolution for Tarawera volcano, New Zealand, and implications for rhyolite magma evolution. *Contrib. Mineral. Petrol.* 67, 1-19.
- Taylor, R., Clark, C. Reddy, S.M., 2012. The effect of grain orientation on secondary ion mass spectrometry (SIMS) analysis of rutile. *Chem. Geol.* 300, 81-87.
- Thomson, S.N., Gehrels, G.E., Ruiz, J., Buchwaldt, R., 2012. Routine low-damage apatite U-Pb dating using laser ablation-multicollector-ICPMS. *Geochemistry Geophysics Geosystems* 13, Issue 2,
- Valley, J. W., Cavosie, A. J., Ushikubo, T., Reinhard, D. A., Lawrence, D. F., Larson, D. J., et al. (2014). Hadean age for a post-magma-ocean zircon confirmed by atom-probe tomography. *Nature Geosci.* 7, 219–223.
- Vazquez, J.A., Reid, M.R., 2004. Probing the accumulation history of the voluminous Toba magma. *Science* 305, 991-994.
- Vorhies, S.H., Ague, J.J., Schmitt, A.K. (2013). Zircon growth and recrystallization during progressive metamorphism, Barrovian zones, Scotland. *American Mineralogist* 98(1), 219-230.
- Watt, G.R., Griffin, B.J., Kinny, P.D., 2000. Charge contrast imaging of geological materials in the environmental scanning electron microscope. *American Mineralogist* 85, 1784–1794.
- Watson, E.B., 1996. Dissolution, growth and survival of zircons during crustal fusion; kinetic principles, geological models and implications for isotopic inheritance. *Geol. Soc. America, Spec. Pap.* 315, 43-56.
- Watson, E. B., Harrison, T. M., 1983. Zircon saturation revisited: temperature and composition effects in a variety of crustal magma types. *Earth Planet. Sci. Lett.* 64, 295–304.
- Wendt, I., Carl, C., 1991. The statistical distribution of the mean squared weighted deviation. *Chem. Geol., Isot. Geosci. Sect.* 86, 275–285.
- White, L.T., Ireland, T.R., 2012. High uranium matrix effect in zircon and its implications for SHRIMP U/Pb age determinations. *Chem. Geol.* 306-307, 78-91.

- Wiedenbeck, M., Allé, P., Corfu, F., Griffin, W., Meier, M., Oberli, F., von Quadt, A., Roddick, J.C., Spiegel, W., 1995. Three natural zircon standards for U-Th-Pb, Lu-Hf, trace element and REE analyses. *Geostand. Newslett.* 19, 1–23.
- Wingate, M.T.D., Compston, W., 2000. Crystal orientation effects during ion microprobe U-Pb analysis of baddeleyite. *Chem. Geol.* 168, 75–97.
- Wotzlaw J.-F., Schaltegger U., Frick D.A., Dungan M.A., Gerdes A., Günther D., 2013. Tracking the evolution of large volume silicic magma reservoirs from assembly to supereruption. *Geology* 41, 867–870.
- Wotzlaw J.F., Hüsling S.K., Hilgen F.J., Schaltegger U., 2014. Testing the gold standard of geochronology against astronomical time: High-precision U-Pb geochronology of orbitally tuned ash beds from the Mediterranean Miocene. *Earth Planet. Sci. Lett.* 407, 19–34.
- Zack, T., Stockli, D.F., Luvizotto, G.L., Barth, M.G., Belousova, E., Wolfe, M.R., Hinton, R.W., 2011. In situ U–Pb rutile dating by LA-ICP-MS: ^{208}Pb correction and prospects for geological applications. *Contributions to Mineralogy and Petrology* 162(3), 515–530.
- Zeh, A., Ovtcharova, M., Wilson, A.H., Schaltegger, U., 2015. The Bushveld Complex was emplaced and cooled in less than one million years - results from zirconology and tectonic implications. *Earth Planet. Sci. Lett.*, in press.

Figures:

Fig. 1: Concordia diagram of two c. 7.24–7.26 Ma old zircons showing the effect of different corrections during the CA-ID-TIMS procedure on the precision and the accuracy of the result; the grey band describes the uncertainty of the position of the concordia curve due to the decay constant uncertainties. a) effect of common-Pb correction: blue ellipses: zircon with $\text{Pb}_{\text{rad}}/\text{Pb}_{\text{com}} = 21.0$; red ellipses: zircon with $\text{Pb}_{\text{rad}}/\text{Pb}_{\text{com}} = 6.7$. Three ellipses are shown with different Pb_{com} isotope compositions from left to right $^{206}\text{Pb}/^{204}\text{Pb} = 18.70, 18.45, 18.20$, respectively, and $^{207}\text{Pb}/^{204}\text{Pb} = 15.75, 15.60, 15.45$, respectively; the Pb_{com} isotope composition does not significantly influence the $^{206}\text{Pb}/^{238}\text{U}$, but does affect the $^{207}\text{Pb}/^{235}\text{U}$.

(b) same two zircons as above, before (below the concordia) and after (concordant) correction for initial ^{230}Th disequilibrium (Schärer 1984) using $D_{\text{Th/U}} = 0.16$ to calculate $\text{Th}/\text{U}_{\text{source}}$. The corrected uncertainty ellipses contain 50% uncertainty of the $\text{Th}/\text{U}_{\text{source}}$, propagated onto the final date after McLean et al. (2011). Example from Wotzlaw et al. (2014; zircons MDC7_z6 and z10).

Fig. 2: Compilation of all R33 reference zircon data (Black et al 2004) from the University of Geneva isotope laboratory, measured between 2004 and 2014 with different tracer

solutions and different mass spectrometers equipped with different secondary electron multipliers (SEM's). The period 2004-2006 contains data measured on MAT262 at ETH Zürich (ETP-SEM) and TRITON at UNIGE (MasCom1-SEM), with a ^{205}Pb - ^{235}U tracer; data measured during the period 2007-2011 used an Earthtime (ET) ^{205}Pb - ^{233}U - ^{235}U tracer, measured on a Triton with a MasCom-2 SEM; the data from 2012-2014 were measured with an ET ^{202}Pb - ^{205}Pb - ^{233}U - ^{235}U tracer on a Triton with a MasCom3-SEM.

Fig. 3: Standard SIMS sample holder geometry for the CAMECA ims1270/1280 showing $^{206}\text{Pb}/^{238}\text{U}$ ages determined on fragments of reference zircon z6266 mounted on mount IP222 (Stern and Amelin, 2003). The random distribution indicates the absence of bias relative to the position within the sample mount (XY-effect) when targets are located within the 15 mm “bullseye” of the mount; XY effects close to the window edge are particularly problematic for high-precision stable isotope analyses, and are mitigated by large sample holder designs (Peres et al., 2012). (B) Histogram and relative probability for $^{206}\text{Pb}/^{238}\text{U}$ ages in (A) indicating the reproducibility for a linear Pb/U RSF vs. UO^+/U^+ calibration based on analysis of reference zircon z6266 using the University of California Los Angeles (UCLA) CAMECA ims1270. Average sputter rate for this experiment is indicated in $\mu\text{m}^3/\text{s/nA O}^-$.

Fig. 4: Schematic of the UCLA CAMECA ims1270 large magnet radius ion microprobe (A) with types of quantitative SIMS analysis used in geochronology: spot mode (B; CL image with typical spot dimensions overlain), depth profiling (C; surface map of unsectioned zircon with SIMS crater on prism face), scanning ion imaging SII (D; $^{49}\text{Ti}^+/\text{SiO}^+$ secondary ion maps overlain onto a Hadean zircon surface image showing high-Ti domains in red associated with fractures), and direct ion imaging DII using the ims1270 channel plate (E; $^{90}\text{Zr}^+$ secondary ion distribution of a zircon with a quartz inclusion in the center of the image; image generated from an accumulated channel plate signal; white square indicates outline of the field aperture).

Fig. 5: Apparent $^{206}\text{Pb}/^{238}\text{U}$ date vs. U abundance for zircons from Tasmanian dolerites analysed by SHRIMP RG (A; White and Ireland, 2012) and CAMECA ims1270 at UCLA (B) relative to the Temora reference zircon. The legend shows the range of the calibration parameter UO^+/U^+ relative to Temora. Gray dashed hockey-stick line schematically represents unbiased low-U analyses in agreement with other radiometric

age determinations for Tasmanian dolerite of ~175 Ma and the apparent age increase at U >2500 ppm (after Fig. 1 in White and Ireland, 2012).

Fig. 6: Probability density distribution (PDD) curves of U-Th zircon crystallization ages for four sequential rhyolite eruptions from Tarawera volcano (Taupo volcanic zone, New Zealand). Model ages are based on two point isochrons using zircon and melt (from whole-rock analysis) compositions. Numbers of individual crystal face, interior (after grinding to ~15 μm depth), and core (in equatorial section at ~50 μm depth) dates are indicated for each curve. Eruption ages (horizontal bars with volcano symbol) are based on ^{14}C ages. Interior ages linked to rim ages of the preceding eruption indicate high probabilities ($P = 0.10 - 0.54$) of similarity suggesting consecutive overgrowth. Horizontal arrows indicate the time lapse Δt between major peaks in rim and interior age distributions, translating into integrated growth rates of $\sim 10^{-13}$ to 10^{-15} cm/s. Note that not only the population, but also individual zircon crystals can record episodic crystallization over time-spans $>10^5$ a. Data from Storm et al. (2011) and Klemetti et al. (2011).

Fig. 7: Age and compositional zonation revealed by depth-profiling of Kaharoa zircon (grain KaT2z3 in Storm et al., 2011; 2014). Parallel depth profiles were acquired on unpolished crystal faces (A); the side opposite to the analyzed crystal face was sectioned to ~15 μm depth and imaged by CL (B). U-Th age and U concentration depth profiles (C); Ti concentrations with model Ti-in-zircon temperatures using $a\text{TiO}_2 = 0.5$ and $a\text{SiO}_2 = 1$ (D); and Zr/Hf as indicator for temperature-dependent zircon fractionation (E). The excursion to high-T (and more primitive melt compositions indicated by low U and high Zr/Hf) after ca. 45 ka is interpreted as local rejuvenation of the crystal storage reservoir following the Rotoiti caldera-forming eruption which was followed by the eruption of comparatively hot and primitive intra-caldera rhyodacites (see Storm et al., 2014, for references).

Fig. 8: Examples of age-ranked $^{206}\text{Pb}/^{238}\text{U}$ dates showing different degrees of age dispersion (data from Broderick, 2014). a) sample with statistically significant age cluster (MSWD = 1.6, within the range of acceptable values for $N=10$; Wendt and Carl 1991) and 2 xeno- or antecrystic zircons with ~250 ka older age ; b) sample showing a larger age dispersion over 184 ± 83 ka; the probability density distribution (PDD) curve indicates two major phases of zircon crystallization at ~42.6 and ~42.5 Ma; c) set of 9 $^{206}\text{Pb}/^{238}\text{U}$

dates indicating an age scatter over 205 ± 86 ka, showing an additional peak of zircon crystallization at ~ 42.45 Ma.

Fig. 9: (a) EBSD (left) and U-Pb data (right) from a ductile zircon crystal from a lower crustal mafic mylonite xenolith, illustrating the role of structural state on U-Pb concordance. The central axis of the crystal has experienced complete resetting of the U-Pb chronometer after deformation resulting in up to 35° rotation of the crystal lattice. Crystal is ca. $100\mu\text{m}$ across (Figures from Moser et al., 2009, reproduced with permission from Elsevier Science). (b) CCI (left) and BSE (right) images of a dolostone from the Bunter Formation, North Sea. The CCI image shows dolomite cores with evidence of partial dissolution surrounded by new concentric growth material. This illustrates the ability of CCI to resolve complexity in crystal structures aiding targeting for high spatial resolution in-situ analysis. Scale bar in both images is $100\mu\text{m}$. Images courtesy of Jeremy Rushton, BGS, for the Bunter Properties Project.

Fig. 10: In-situ analysis of micro-zircons from a Northern Madison Range (Montana) metamorphic mafic dike. (A) Micro-zircon crystals in backscatter-image showing crystals completely enclosed in quartz (z272), intersected by an annealed fracture in quartz (z271), and interstitial at grain boundaries between quartz and garnet (z274). Inset illustrates primary beam spot size ($\sim 20\mu\text{m}$) and dimensions of field aperture ($\sim 10\mu\text{m}$) limiting secondary ion acceptance. (B) Concordia diagram of SIMS analyses highlighting spots in (A). Discordance is high for crystals located at grain boundaries, whereas those hosted in intact quartz are concordant. These results suggest that radiation damage alone is insufficient to explain discordant vs. concordant behaviour of zircon, and indicates that shielding can mitigate Pb-loss (Ault et al., 2012).

Fig. 11: SIMS depth profile for zircon from the sillimanite-K-feldspar zone sample 286B (Glen Muick, Barrovian, Scotland). (A) $^{206}\text{Pb}/^{238}\text{U}$ dates and percent concordance between $^{207}\text{Pb}/^{235}\text{U}$ and $^{206}\text{Pb}/^{238}\text{U}$ dates and (B) Th/U. (C) backscatter electron image of depth-profiled zircon (with SIMS analysis spots in center of crystal showing up as bright areas due to charging where the conductive Au coat has been removed). The analyzed metamorphic overgrowth is only $\sim 1.5\mu\text{m}$ thick and is preceded by a spike in Th/U interpreted to be due to Th mobilization during partial melting. Crystal interior is an inherited core, likely of metamorphic origin (Vorhies et al., 2013)

Fig. 12: (a) Model using middle and heavy rare earth element variations in ID-TIMS dated zircon as a result of titanite fractionation, used to calculate percentage of crystal in the crystallizing Fish Canyon Tuff magma over 420 ka; (b) modelled compositional trends for a titanite-free fractionation assemblage (grey points) and for an assemblage containing 0.4% titanite. The model documents near-solidification with 78% crystals at 28.4 Ma and subsequent rejuvenation of the magma to 40% crystals at 28.2 Ma (modified from Wotzlaw et al., 2013).

Tables

Tab. 1: Charted strengths and weaknesses of the three methods of U-Pb dating. Sources: [1] Schmitt et al. (2010), [2] Frei and Gerdes (2009), [3] Cottle et al. (2009)

Tab. 2: Natural zircon reference materials characterized by ID-TIMS; source of data: [1] Kennedy et al. (2014); [2] Sláma et al. (2008); [3] Black et al. (2003); [4] Black et al. (2004); [5] Jackson et al. (2004); [6] Schaltegger et al., unpubl., in: Boekhout et al. (2012); [7] Wiedenbeck et al. (1995); [8] Schoene et al., (2006); [9] Paces and Miller (1993). Uncertainties are indicated in X/Y format (following Schoene et al., 2006) where available. Data in [1], [2], [6] and [8] are corrected for initial ^{230}Th disequilibrium.

Tab. 1

	ID-TIMS	SIMS	LA-ICP-MS
Absolute age resolution (2σ)	U-Pb high to very high: $\leq 0.1\%$ precision and accuracy	U-Th and U-Pb ca. 1-2 %; very high ($\sim 10^3$ - 10^4 years) for U-Th dating < 300 ka	U-Pb ca. 2% Th-Pb ca. 3%
Spatial resolution	Poor (mixing of age domains in single crystals hardly avoidable)	Excellent (sub- μm in depth profiling); quasi non-destructive	Good (20-30 μm laterally, single μm vertically, depending on analytical system)
Useful yield for U	$< 1\%$ (as UO_2^+)	0.7-1% (as UO^+)	Very variable (0.01-2.8%) depending on type of mass spec*)
Useful yield for Pb	High ($\sim 5\%$), depending on the source of Si-gel	High ($\sim 1\%$) [1]	Intermediate ($\sim 0.2\%$ -0.4%) to high (2%) depending on type of mass spec [2]*)
Time requirements for sample preparation and analysis	Slow (digestion and chemical separation)	Fast (CL imagery, volumetric excavation rate $\sim 0.1 \mu\text{m}^3/\text{sec/nA}$ primary beam) [1]	Very fast (CL imagery, volumetric excavation rate $\sim 0.125 \mu\text{m}^3/\text{pulse}$ at 2.4 J cm^{-3} fluence) [3]
Preferred geologic applicability	Volcanic and plutonic systems of any age	Young volcanic systems with volcanic and plutonic enclaves; Metamorphic systems; Microcrystal and in situ analysis	Detrital provenance studies, young volcanic and plutonic systems, metamorphic systems, in situ analysis

*) Useful yields in % (=ions detected/total number of atoms in sample volume for a species of interest) for U and Pb, respectively; for quadrupole-ICP-MS: 0.01%, 0.01%; for single collector, sector-field ICP-MS: 0.3%, 0.2%; for multicollector ICP-MS: 0.4-2.8%, 0.3-2%.

Tab. 2

Name	Certified age [Ma]	Type of age	Source
AUSZ2	$38.8963 \pm 0.0044/0.012$	$^{206}\text{Pb}/^{238}\text{U}$	[1]
Plešovice	$337.13 \pm 0.06/0.23$	$^{206}\text{Pb}/^{238}\text{U}$	[2]
Temora 1	416.75 ± 0.24	$^{206}\text{Pb}/^{238}\text{U}$	[3]
Temora 2	416.78 ± 0.33	$^{206}\text{Pb}/^{238}\text{U}$	[4]
R33	418.9 ± 0.4	$^{206}\text{Pb}/^{238}\text{U}$	[4]
	419.26 ± 0.39	$^{206}\text{Pb}/^{238}\text{U}$	[4]
GJ-1	608.53 ± 0.37	$^{207}\text{Pb}/^{206}\text{Pb}$	[5]
GJ-1 nr. 67	600.5 ± 0.4	$^{206}\text{Pb}/^{238}\text{U}$	[6]
Harvard 91500	1065.4 ± 0.3	$^{207}\text{Pb}/^{206}\text{Pb}$	[7]
	$1066.4 \pm 0.3/5.0$	$^{207}\text{Pb}/^{206}\text{Pb}$	[8]
	$1063.6 \pm 0.2/0.3$	$^{206}\text{Pb}/^{238}\text{U}$	[8]
AS3	1099.1 ± 0.5	$^{207}\text{Pb}/^{206}\text{Pb}$	[9]
	1099.0 ± 0.7	$^{206}\text{Pb}/^{238}\text{U}$	[9]
	$1098.6 \pm 0.3/5.0$	$^{207}\text{Pb}/^{206}\text{Pb}$	[8]
	$1095.9 \pm 0.2/0.3$	$^{206}\text{Pb}/^{238}\text{U}$	[8]
FC1	1099.0 ± 0.6	$^{207}\text{Pb}/^{206}\text{Pb}$	[9]
	1099.9 ± 1.1	$^{206}\text{Pb}/^{238}\text{U}$	[9]
QGNG	1851.5 ± 0.3	$^{207}\text{Pb}/^{206}\text{Pb}$	[8]
	$1848.7 \pm 0.7/0.9$	$^{206}\text{Pb}/^{238}\text{U}$	[8]

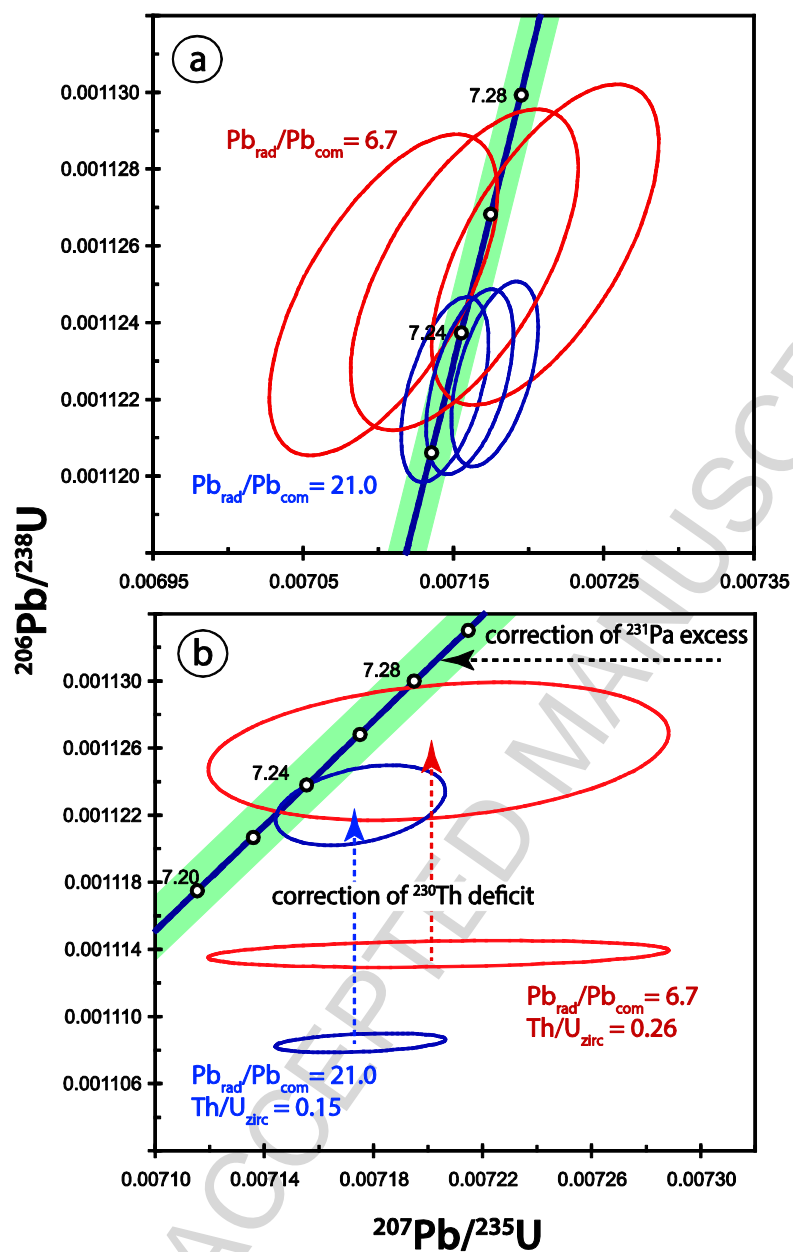


Figure 1

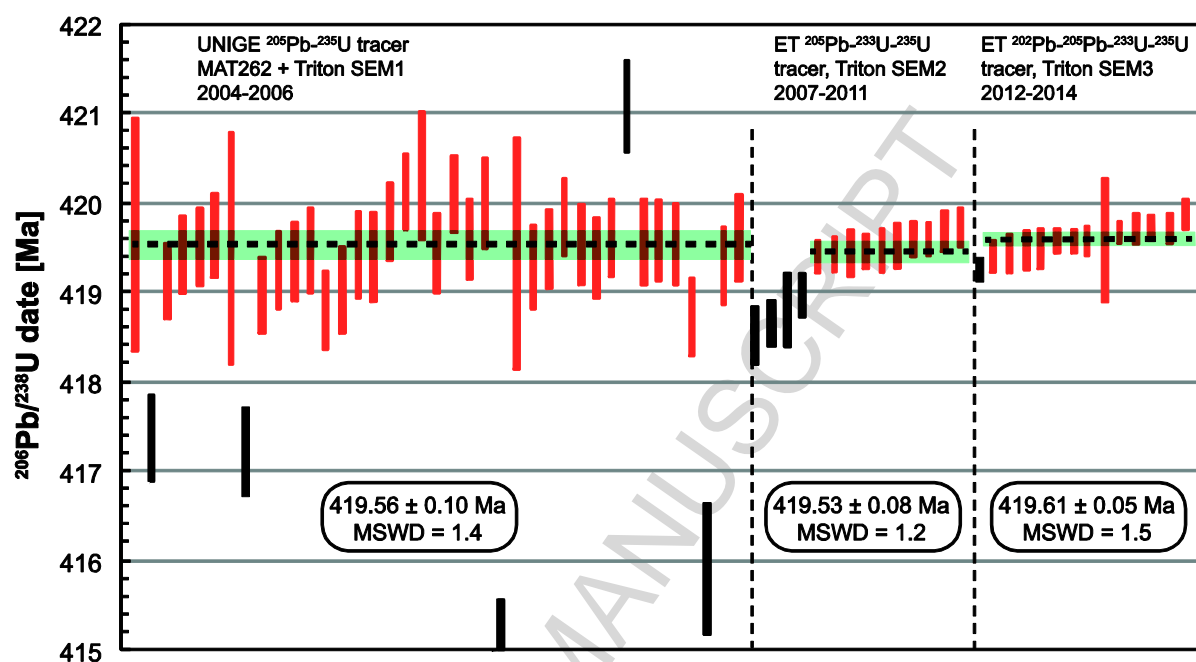


Figure 2

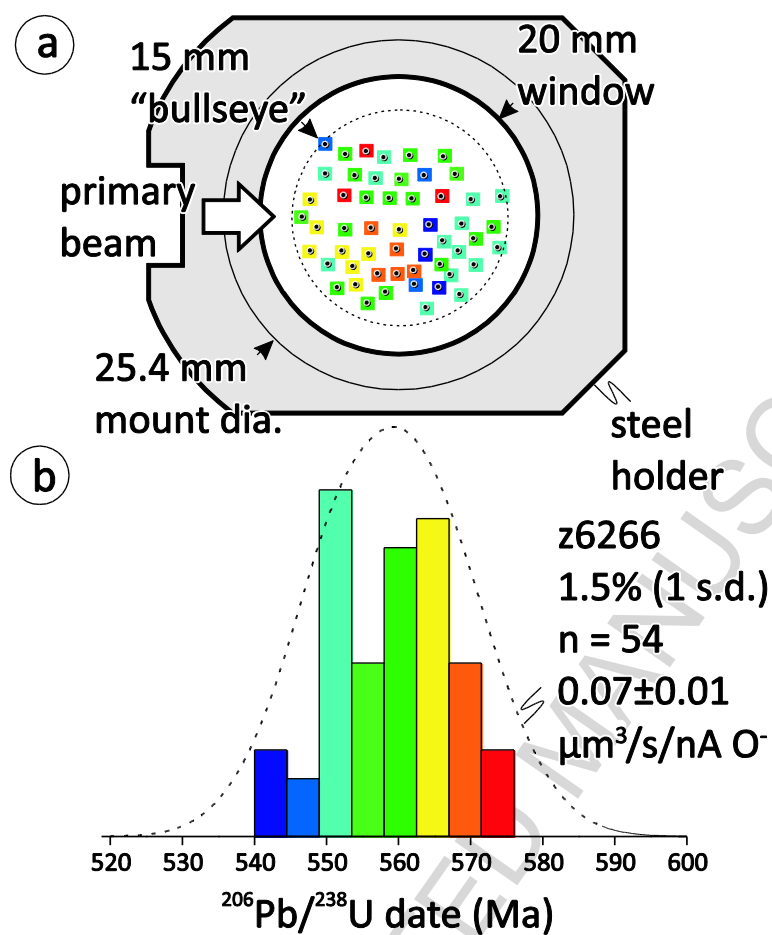


Figure 3

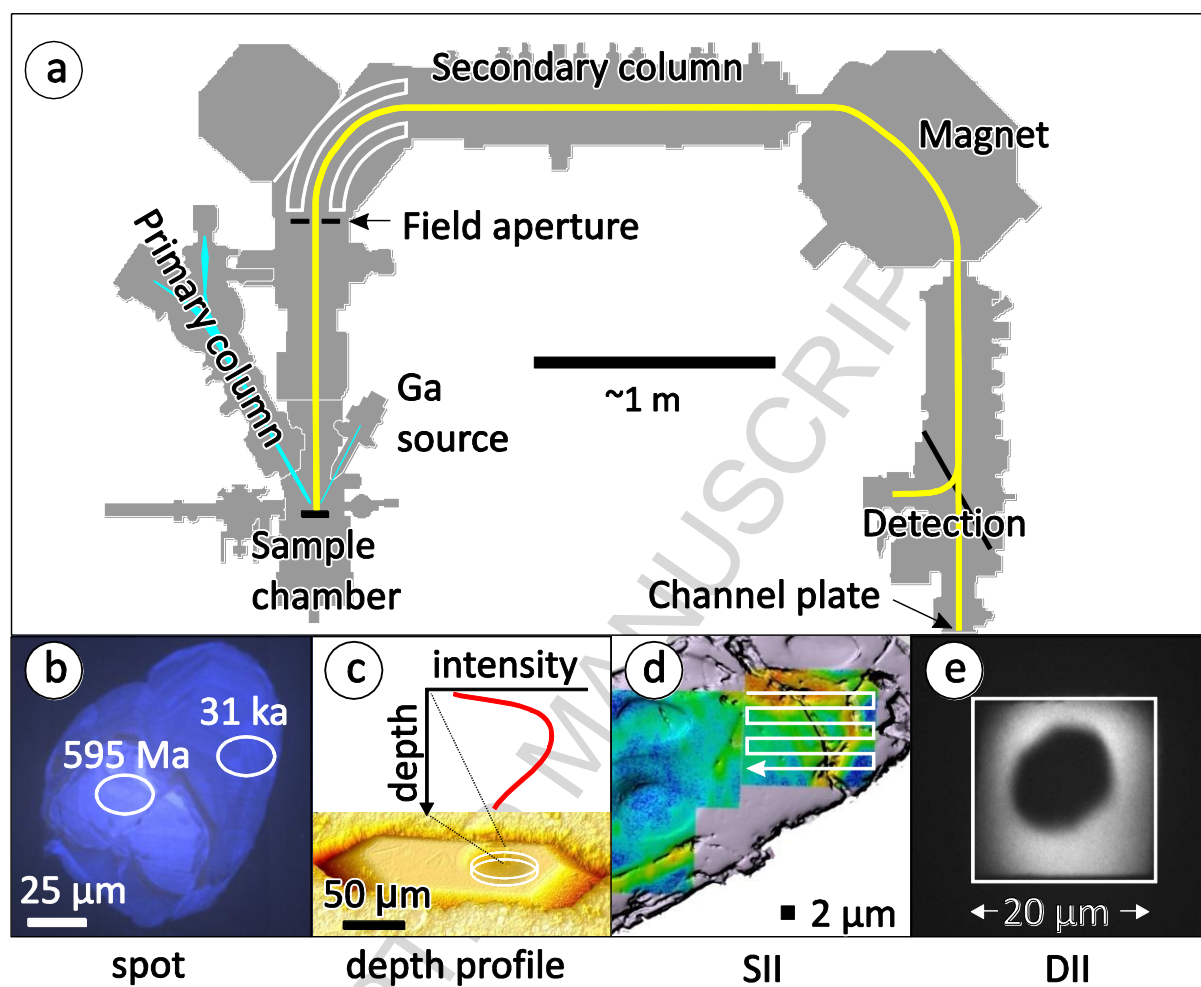


Figure 4

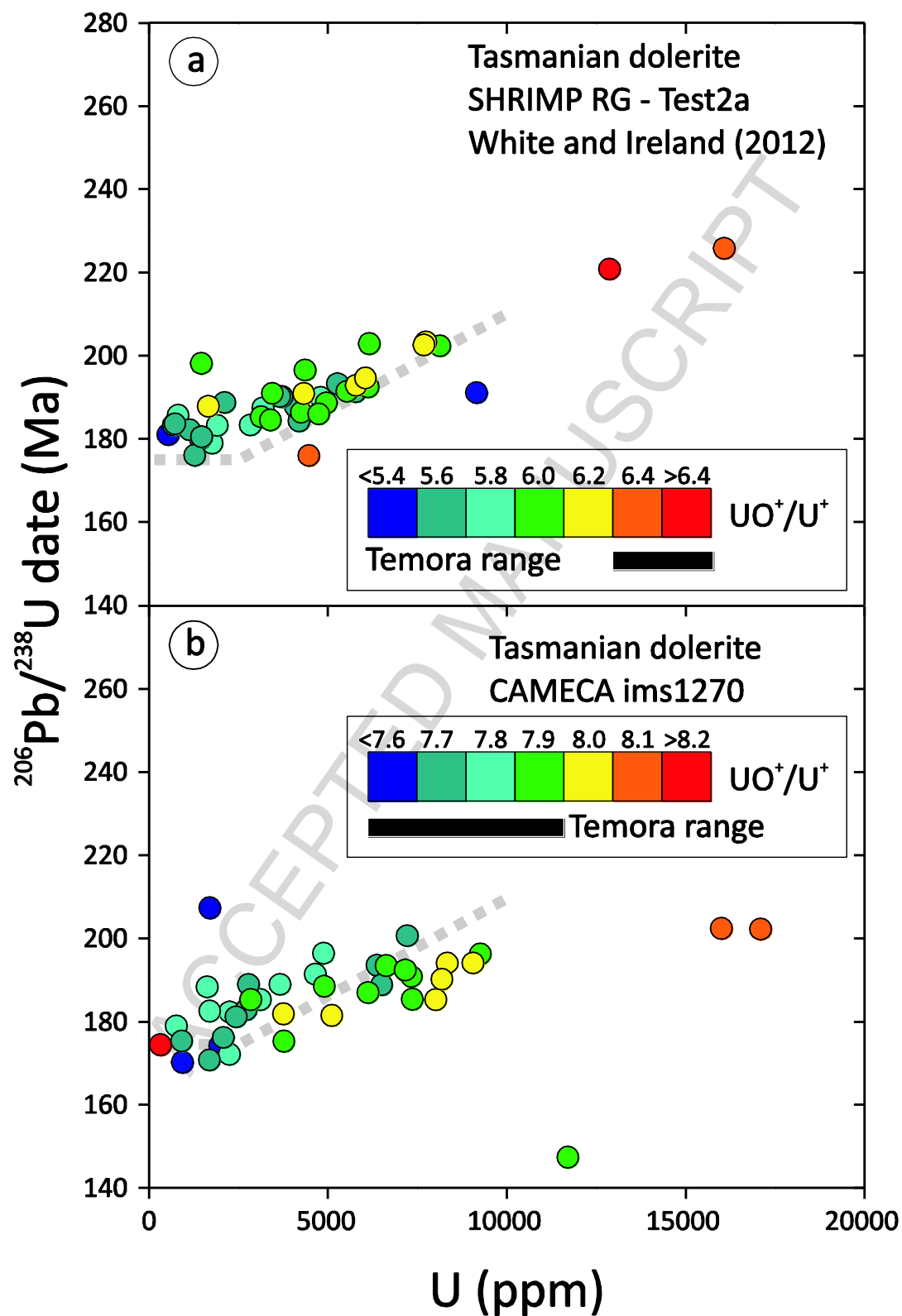


Figure 5

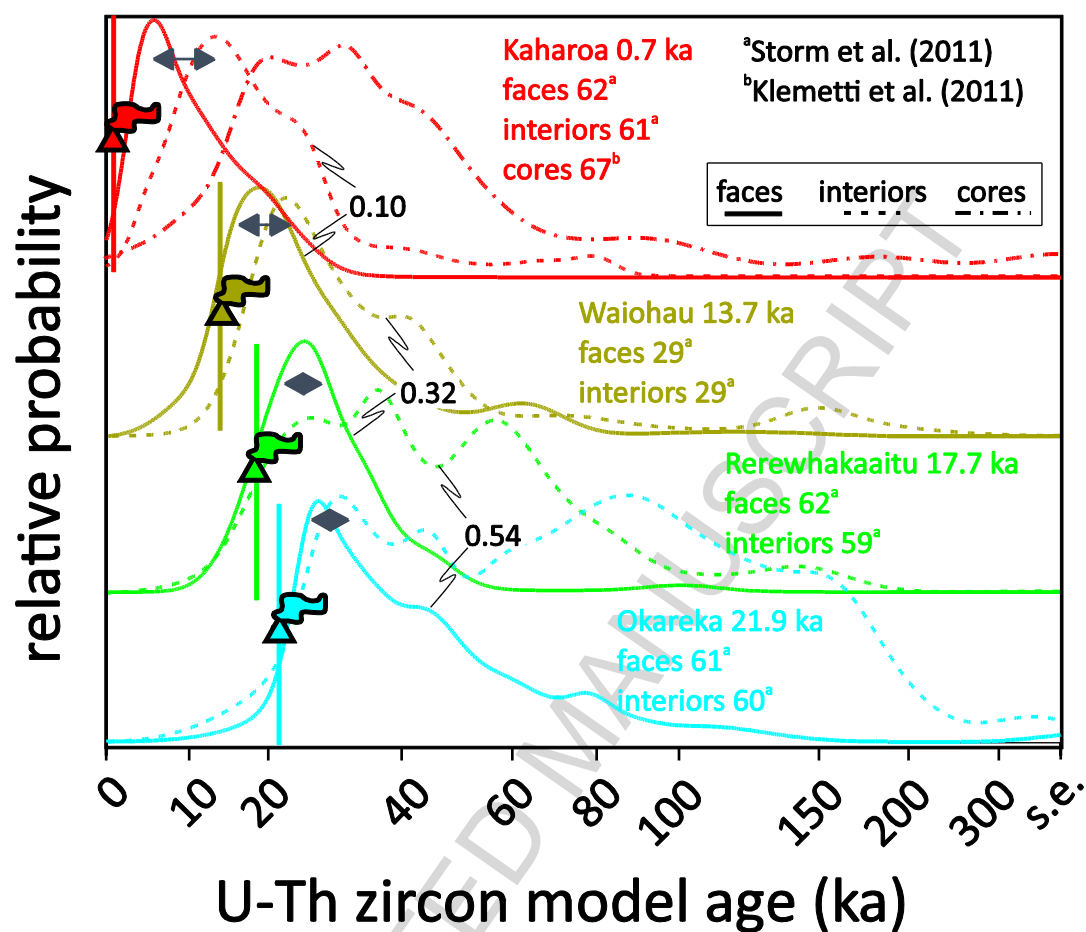


Figure 6

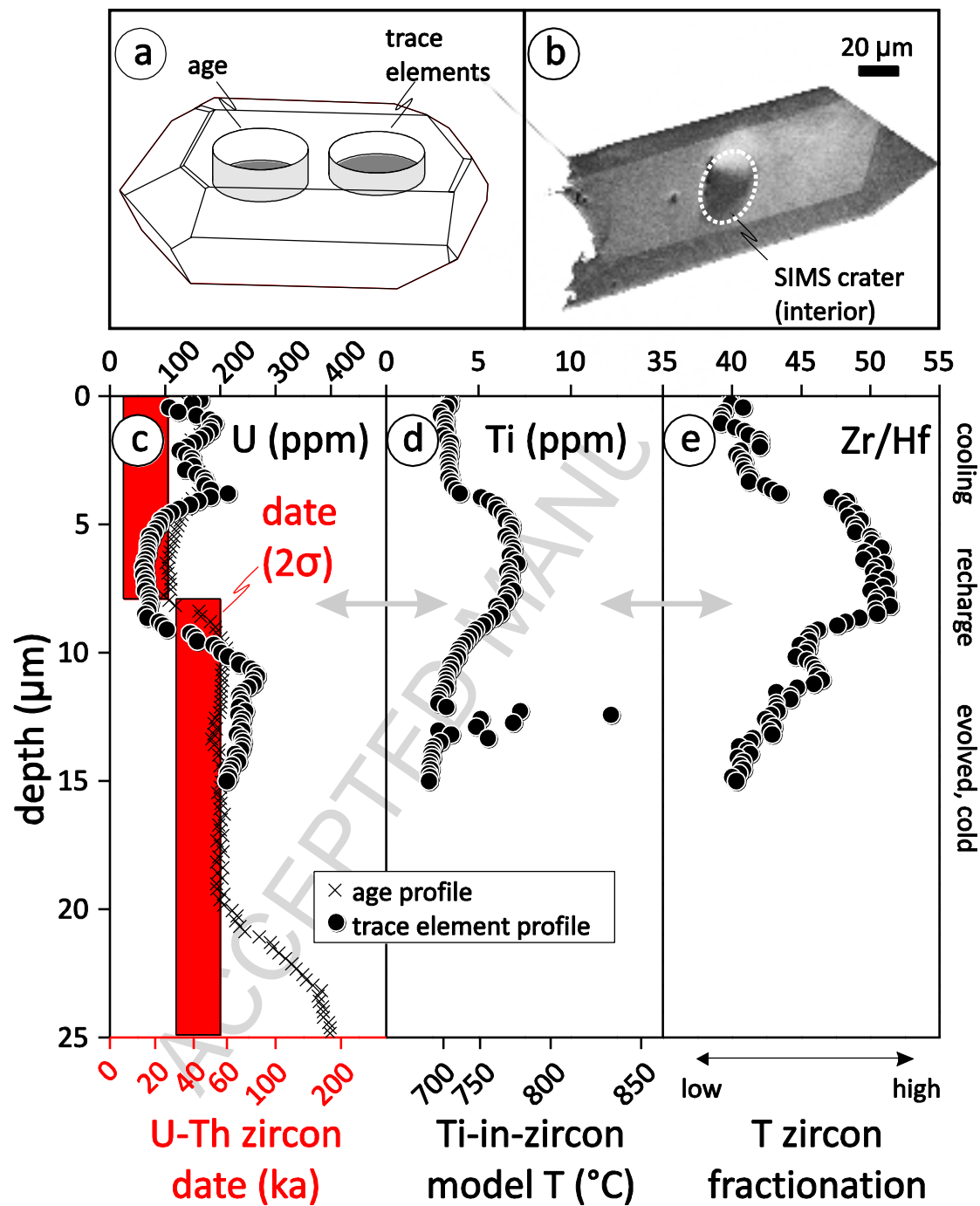


Figure 7

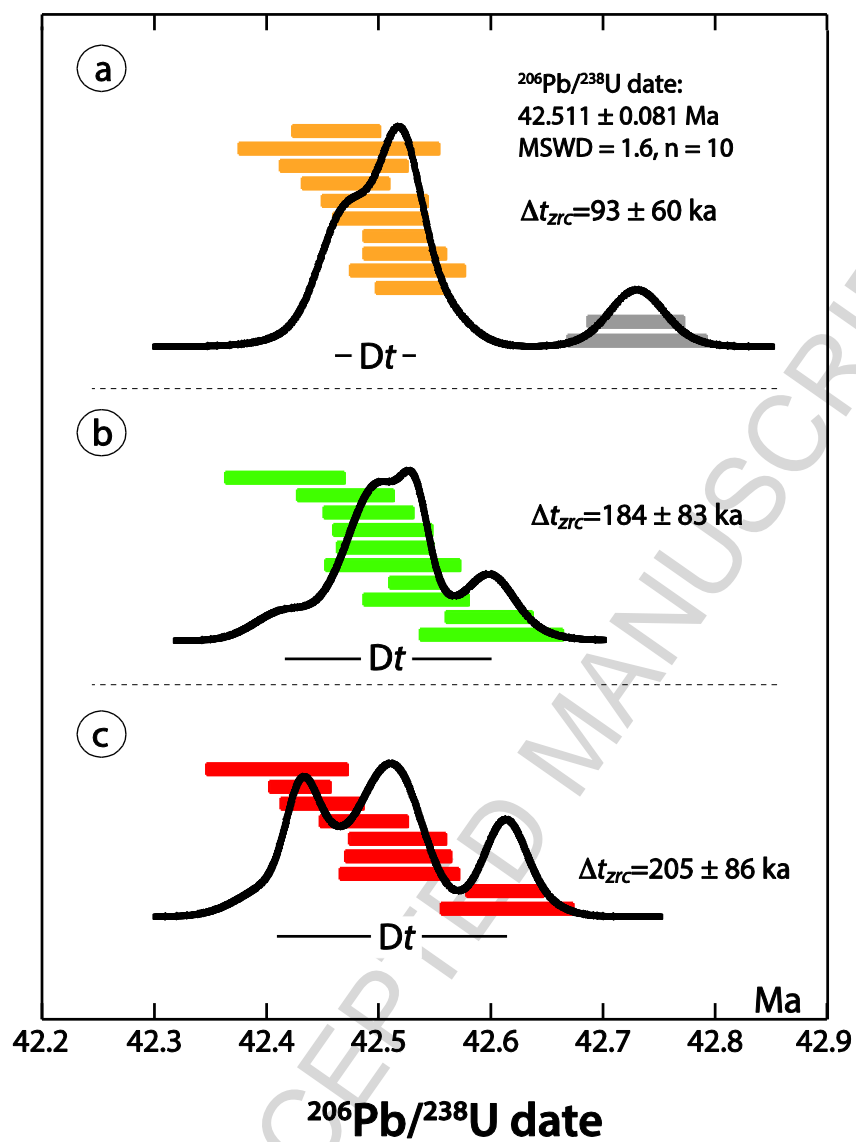


Figure 8

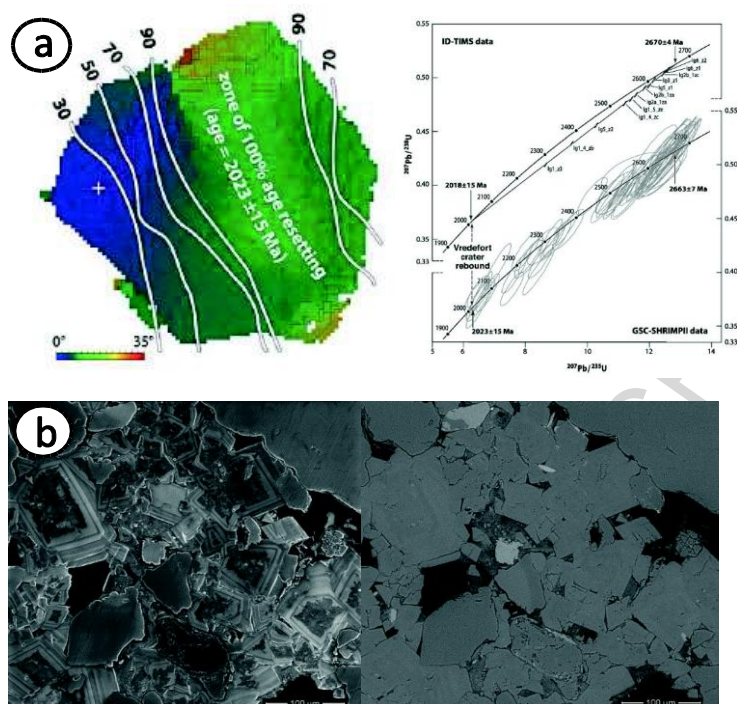


Figure 9

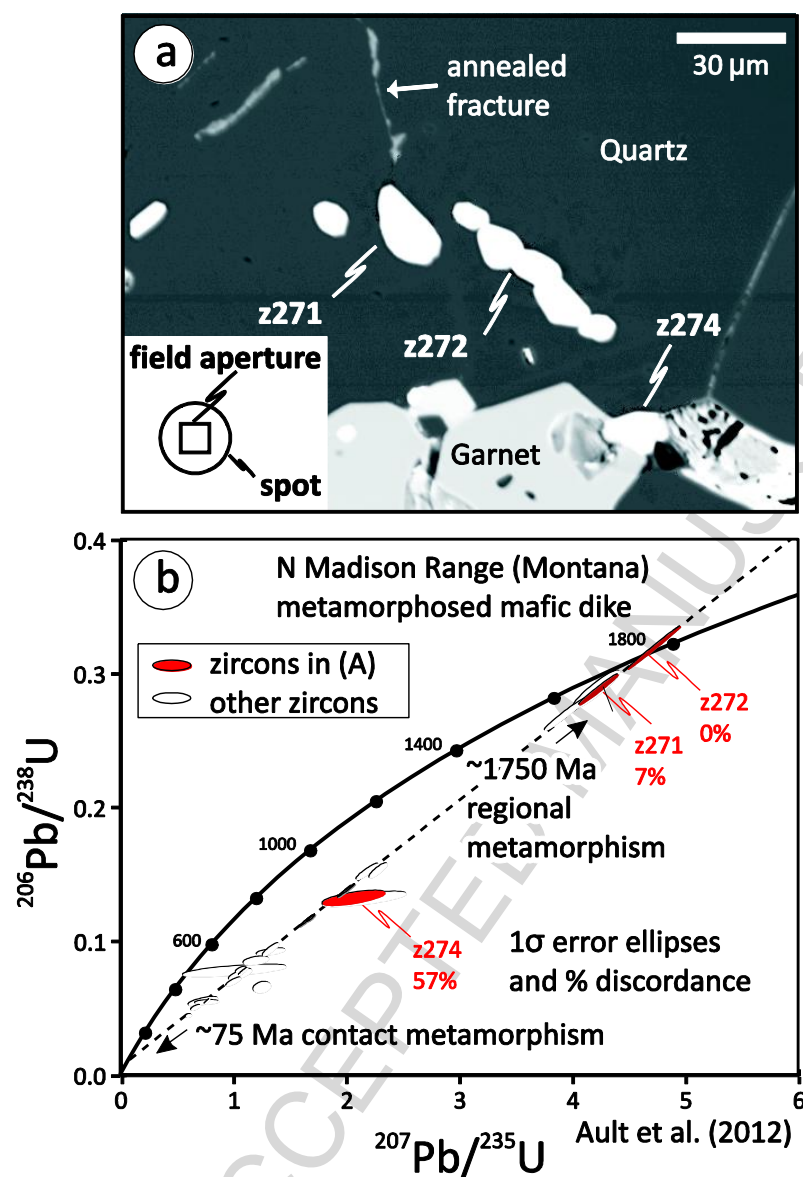


Figure 10

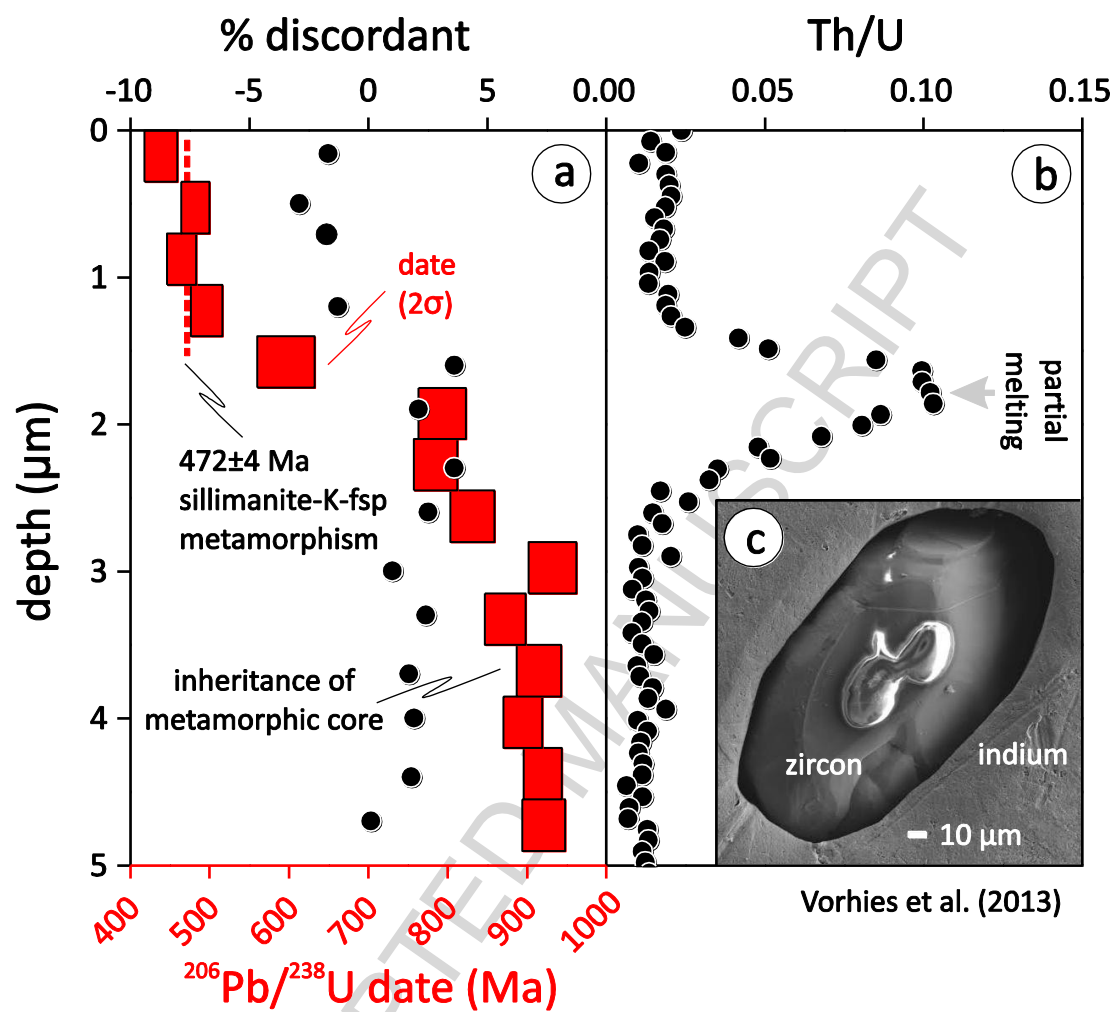


Figure 11

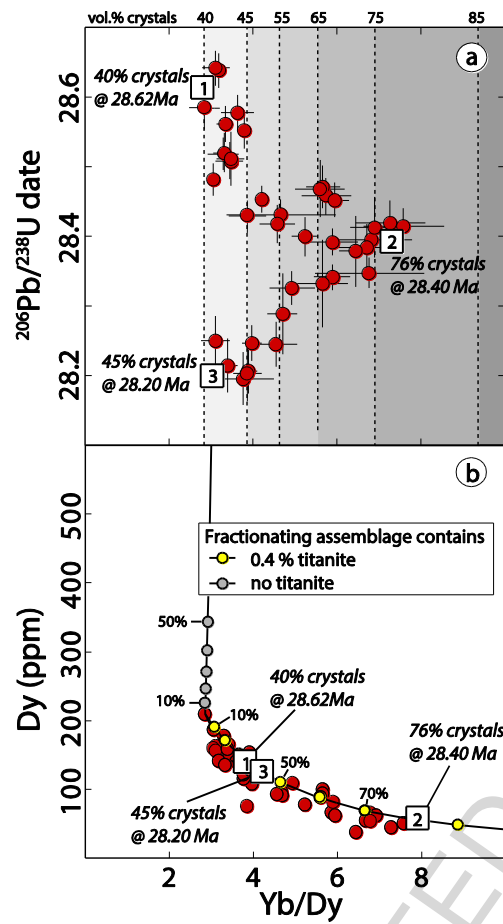


Figure 12